Particle Identification Techniques

ID techniques are based on the detection of particles via their interaction with matter
ionization and excitation (Cherenkov light & Transition Radiation)

ne applicable methods depend strongly on the
article momentum (velocity) domain of interest

π-K identification ranges

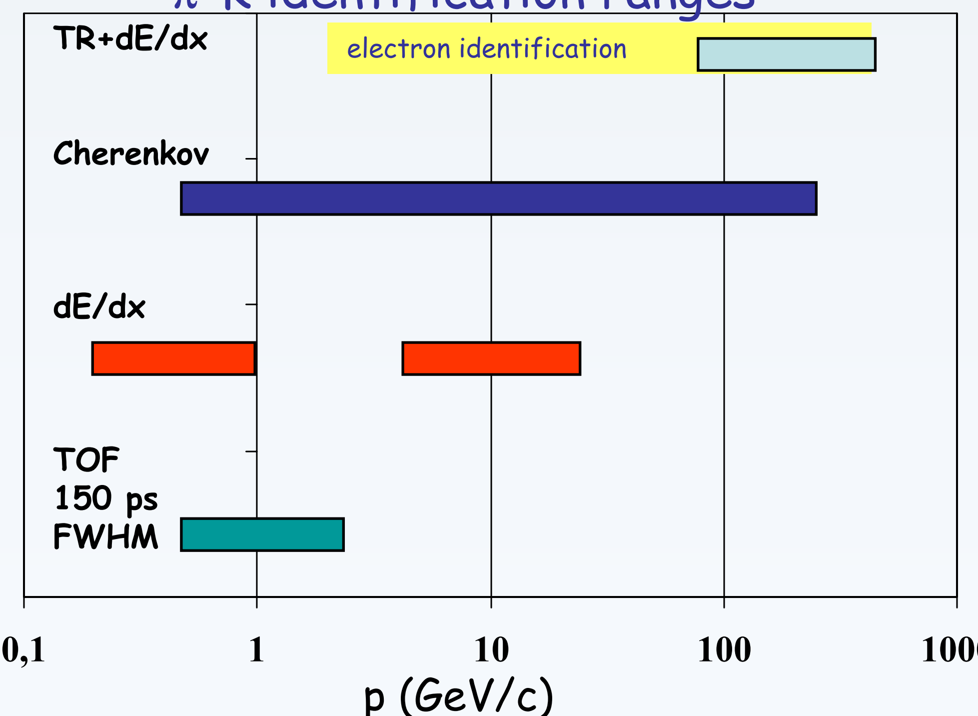

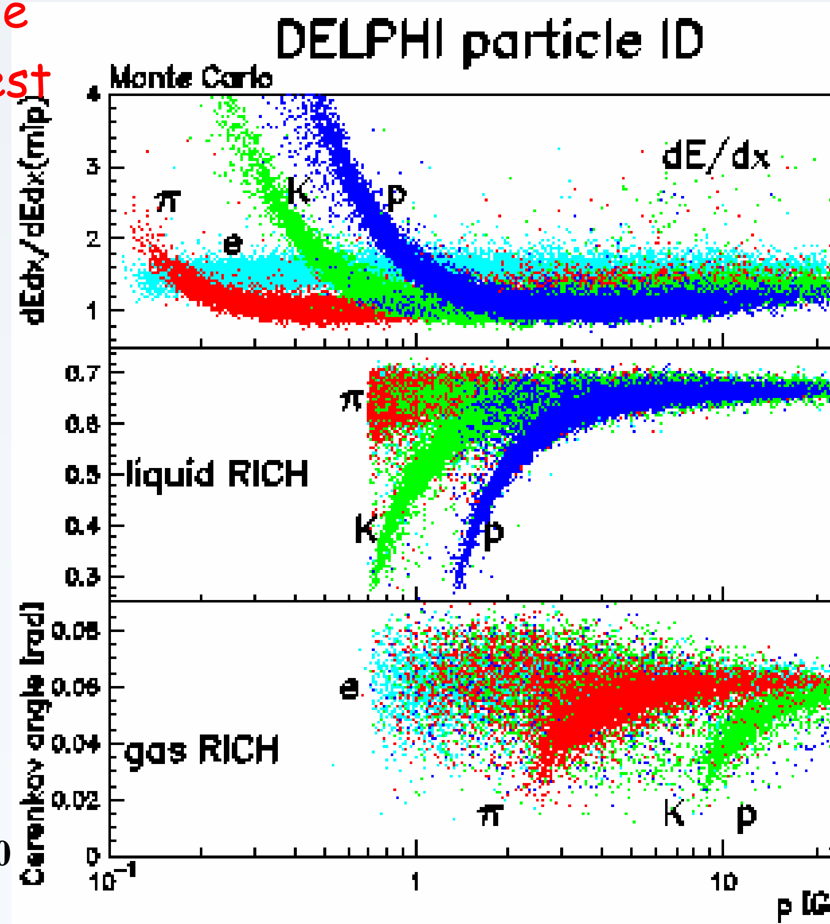

CHERENKOV DETECTORS

Contents

- Cherenkov radiation: history
- Properties of Cherenkov radiation and basic formulae
- Design criteria of RICH detectors
  - ⇒ Separation power
  - ⇒ Detector components
  - ⇒ CsI RICH & ALICE HMPID
  - ⇒ Aerogel RICH
    - ⇒ HERMES
    - ⇒ LHCb

Historical overview

- 1888 - O. Heaviside : a superluminal charged particle in vacuum (!) emits an e.m. radiation
- 1919 - M. Curie: faint blue light from concentrated solutions of radium in water
- 1934 - P. A. Cherenkov: exhaustive series of experiments on visible light emitted by Compton electrons produced by bombarding pure liquids with γ rays
- 1937 - I. M. Frank and I. J. Tamm: classical theory of Cherenkov radiation
- 1940 - V. L. Ginzburg: quantum theory of Cherenkov radiation
- 1951 - J. V. Jelley: first Cherenkov detector finalized to PID in a physics experiment
- 1955 - E. Segre', O. Chamberlain, C. Wiegand and T. Ypsilantis: discovery of antiproton
- 1958 - P. A. Cherenkov, I. M. Frank and I. J. Tamm: Nobel prize for Physics
- 1960 - A. Roberts: first conception of Ring Imaging CHerenkov technique
- 1977 - J. Seguinot and T. Ypsilantis: "imaging" of Cherenkov patterns in a gas detector
- 1993 - First Workshop on RICH detectors, Bari 2-5 June: consecration of the technique

Ring Imaging CHerenkov technique

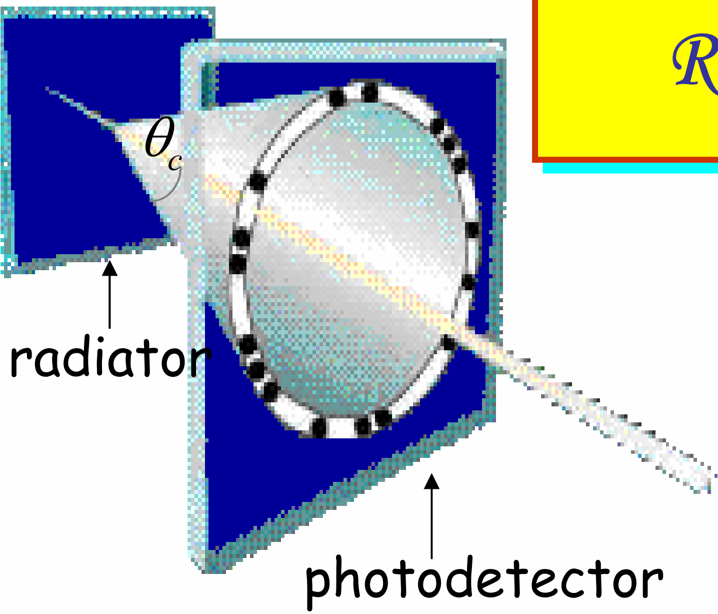

$$\theta_c = \arccos\frac{1}{n(\lambda)\beta}\begin{cases}\gamma_t = \left(1-\frac{1}{n^2}\right)^{-\frac{1}{2}} & \text{energy threshol} \\ \theta_c = \theta_c(\beta) & \end{cases}$$

intrinsic "chromaticity"

dispersion limit

Particle Identification:

Cherenkov angle -> particle velocity

\+

momentum known

$$m = p\sqrt{n^2\cos^2\theta_c - 1}$$

Separationpower:

$$\text{os}\theta = \frac{1}{n\beta} \Rightarrow \left(\frac{\sigma_\beta}{\beta}\right)^2 = (\tan\theta\sigma_\theta)^2 + \left(\frac{\Delta n}{n}\right)^2$$

$$\theta_2 - \theta_1 = n\sigma_{\theta_c}$$

$\Downarrow$ PARTICLE MASS m_1 $\Downarrow$ PARTICLE MASS m_2

$$\sigma_\theta^2 = \sum_i \Delta\theta_i^2 \Rightarrow \sigma_{\theta_c} = \frac{\sigma_\theta}{\sqrt{N_{p.e.}}}$$

minimize maximiz

Cherenkov Light Imaging counters:

detect the maximum number of photons with the best angular resolution

E. Nap

Identificazione di particelle

Ring Imaging CHerenkov counters

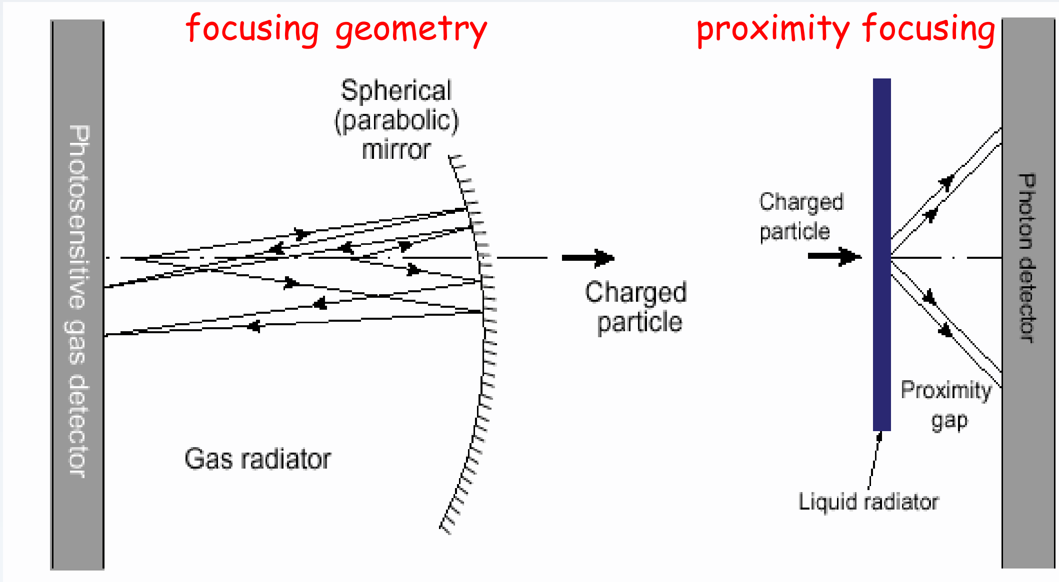

Cherenkov Light Imaging

Detection of Internally Reflected Cherenkov light

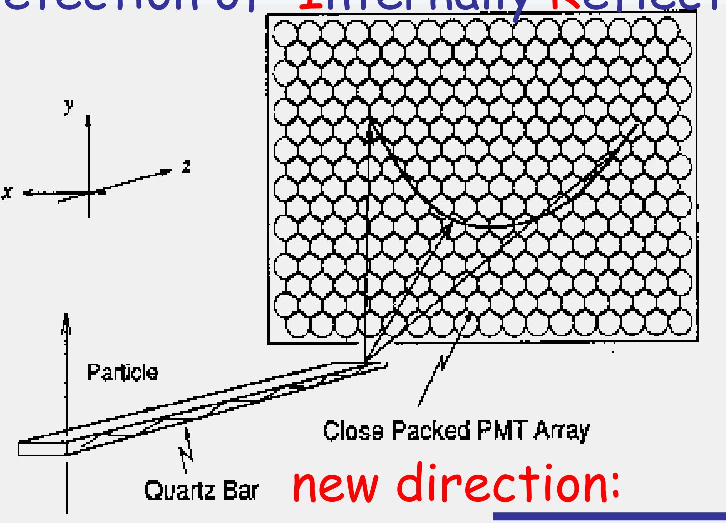

new direction: correct the chromatic error

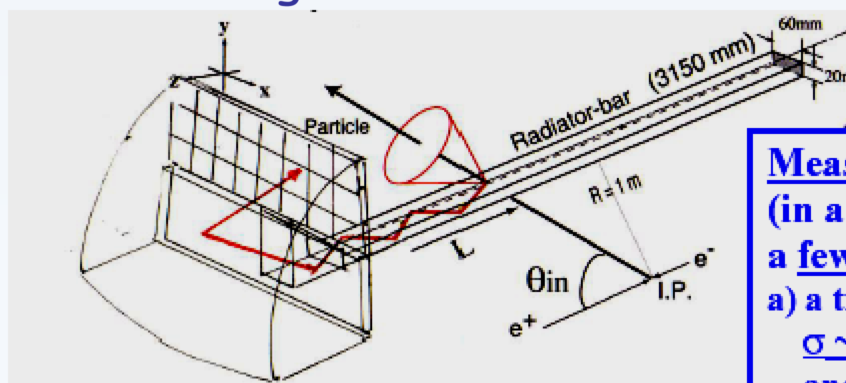

X, Y, Time

(Focusing mirror, quartz matching fluid, Flat panel H-8500 PMT detector)

Measure (in a field of a few Gauss):
a) a time to σ ~ 100ps, and
b) photon position in both x & y.

Intensity distribution-I

Frank and Tamm Equation:

E energy radiated per unit of path dx by a particle of charge Ze in a dielectric medium of refractive index n(ω)

$$\frac{d^2E}{dx\,d\omega} = \frac{Z^2e^2\omega}{c^2}\left(1-\frac{1}{\beta^2 n^2(\omega)}\right)$$

$$\frac{dE}{d\omega} = \frac{Z^2e^2\omega}{c^2}\left(1-\frac{1}{\beta^2 n^2(\omega)}\right)L$$

$$E=\sum_{i=1}^{N}\hbar\omega_i = N\hbar<\omega> \Rightarrow \quad N = 2\pi L Z^2\alpha \int_{\beta n>1}\left(1-\left(\frac{\beta_t(\lambda)}{\beta}\right)^2\right)\frac{d\lambda}{\lambda^2}$$

Electron energy loss, in the visible (λ:400-700 nm
β ~1, in 1 cm of water (n=1.33) ⟶ 500 eV
(ionization ⟶ 2 MeV !!)

Intensity distribution-II

$$N = 2\pi L Z^2 \alpha \int_{\beta n \succ 1} \left(1 - \left(\frac{\beta_t(\lambda)}{\beta}\right)^2\right)\frac{d\lambda}{\lambda^2} \xrightarrow{\beta\approx 1} N(cm^{-1}eV^{-1}) = 370 Z^2\left(1 - \frac{1}{n^2}\right)$$

Material	*Refractive index*	γ_t	$\theta_{max}(^0)$	$N\gamma/(cm\ eV)$
plexiglass	1.48	1.36	44	220
water	1.33	1.56	41.2	160
aerogel	1.01-1.07	27- 4.5	11-25	20-80
argon	1.00059	31	1.8	0.46
helium	1.000033	120	0.47	0.04

energy loss in solids ~ O(keV/cm)
photon yield proportional to Z^2
most of the radiation in the UV

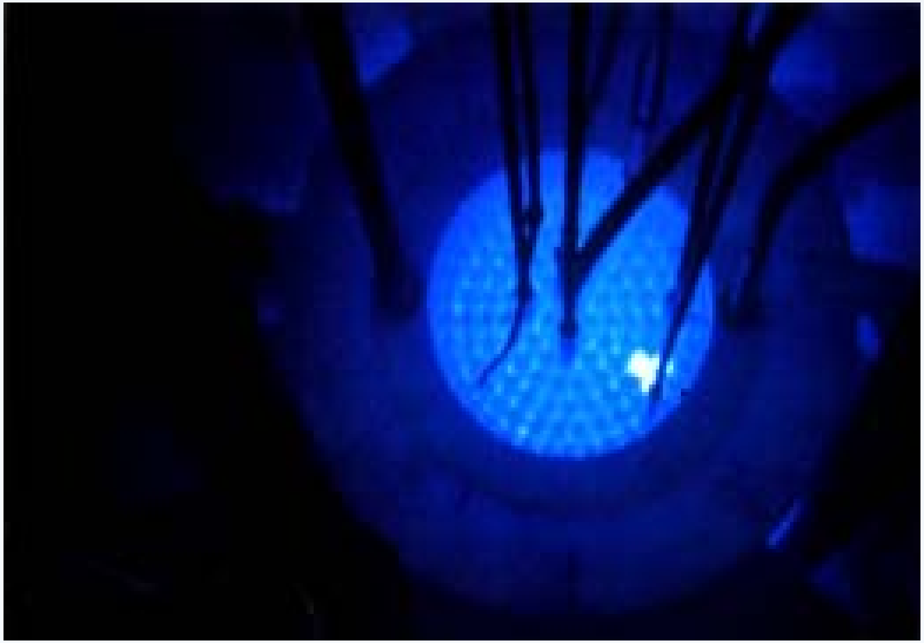

Detected Photoelectrons

$$N = 2\pi L Z^2 \alpha \int_{\beta n \succ 1} \left(1 - \left(\frac{\beta_t(\lambda)}{\beta}\right)^2\right) \frac{d\lambda}{\lambda^2}$$

$$N(cm^{-1} eV^{-1})_{\beta \approx 1} = 370 Z^2 \left(1 - \frac{1}{n^2}\right)$$

too few Cherenkov photons

$\varepsilon = \text{single photoelectron detection efficiency}$

$\text{Q} = \text{photoconverter Quantum Efficiency}$

$\text{T} = \text{transmission of radiator, gas and windows}$

$\text{R} = \text{mirror reflectivity}$

$$\text{N}_0 = \text{figure of merit} = \frac{2\pi\alpha}{\text{h}} \int \varepsilon \cdot \text{Q} \cdot \text{T} \cdot \text{R} \cdot \text{dE}$$

$$N_{pe} = \text{mean number of detected photoelectrons} = \text{N}_0 \text{ L} \sin^2\theta$$

The number of photo-electrons N_{pe} is even smaller !

$$\sin^2\theta_{\max} = \frac{1}{\gamma_t^2} \Rightarrow \text{N}_{\text{pe-max}} = \frac{\text{N}_0 \text{L}}{\gamma_t^2}$$

Photon Detector Requirements

- Large area coverage with single photon sensitivity
- High "effective" efficiency
  - Active-area fraction > 70%
- High granularity
- Rate capability
- Reliability and long term ageing resistance
- Timing resolution (σ ~100 ps)
- Affordable procurement and operating costs

In red, requirements very peculiar to Cherenkov light Imaging applications

Examples:

Large Surface Sensitive to Single Photons

HADES-GSI

Photon Detector :

- CH_4 MWPC – CaF_2 windows
- CsI photo-cathode
- 28 600 pads

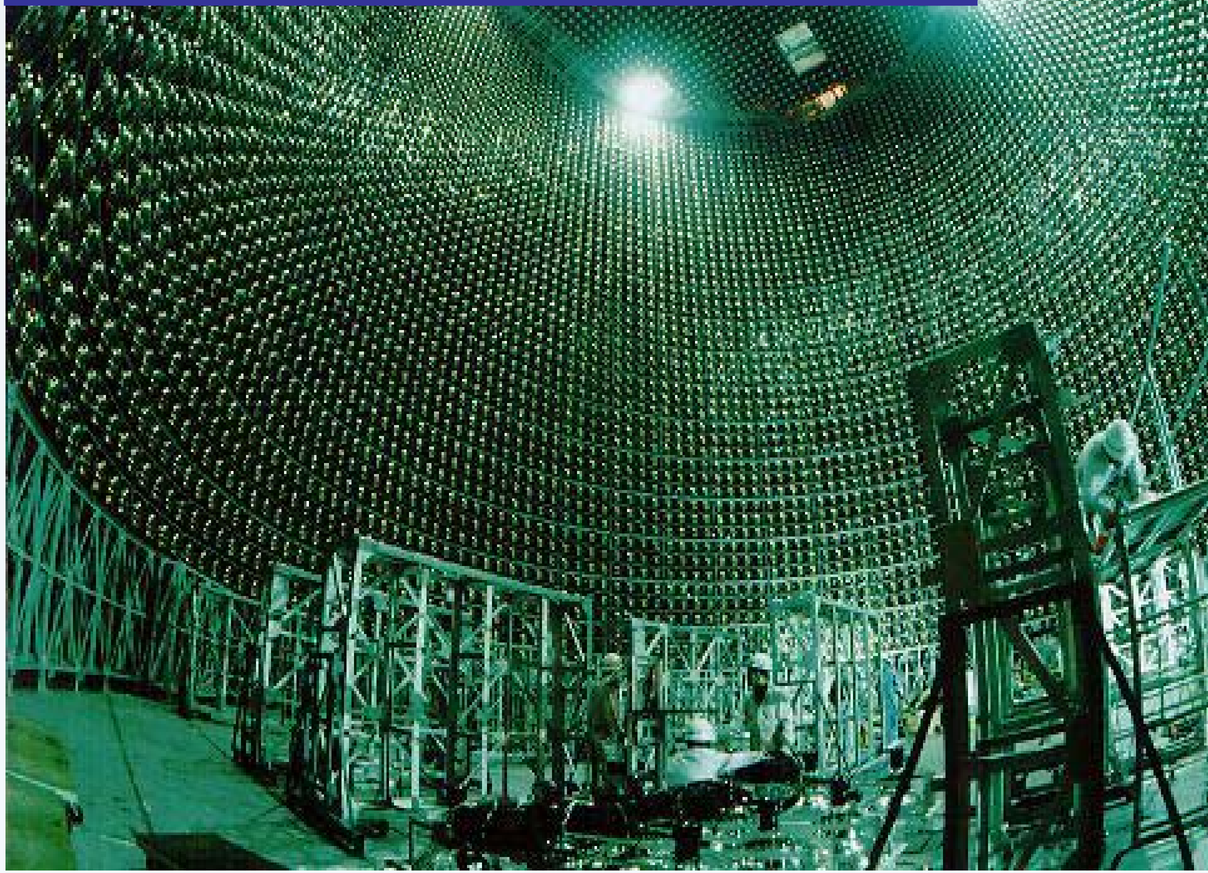

Super-Kamiokande

50 000 ton water

11000 PMTs 50cm ∅

Gaseous photon detector

PHOTOELECTRIC ABSORPTION

as photoionization
as volume: photosensor (TMAE or TEA)
+ carrier (CH_4 or C_2H_6)

photoelectric effec
gas volume: CH

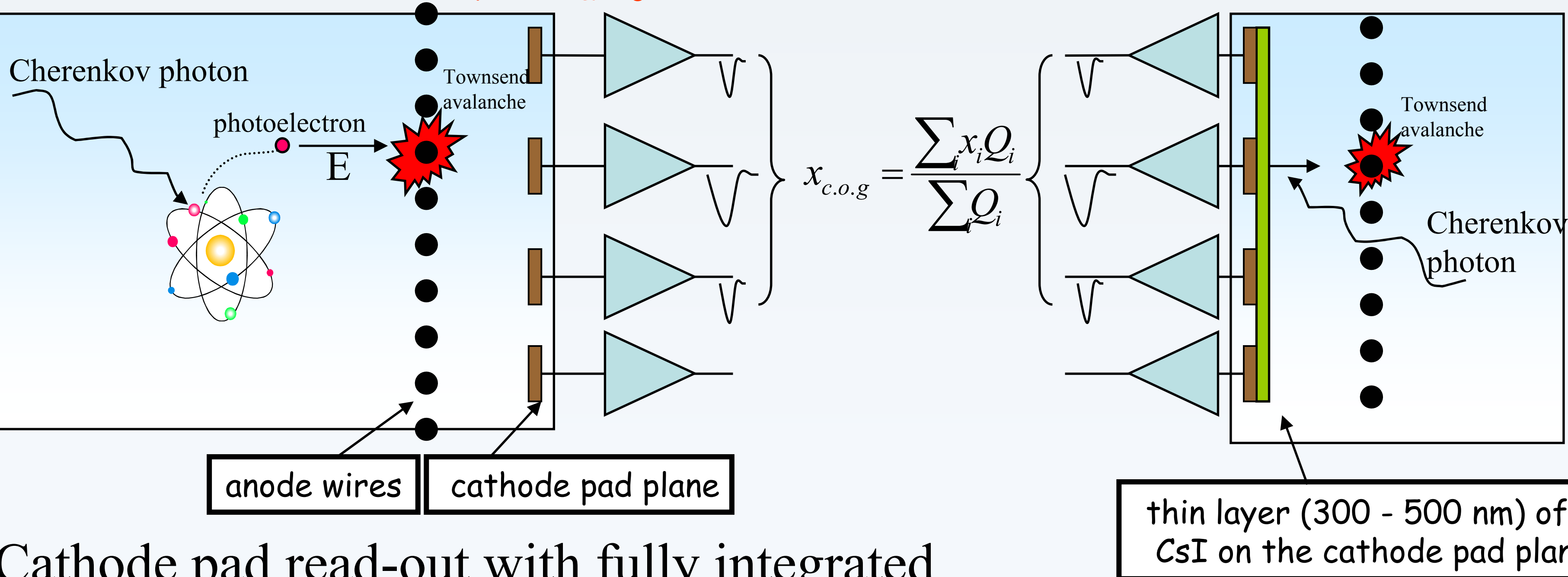

Cathode pad read-out with fully integrated electronics over the back side ➔ reduced cabling, less dead space

Identificazione di particelle

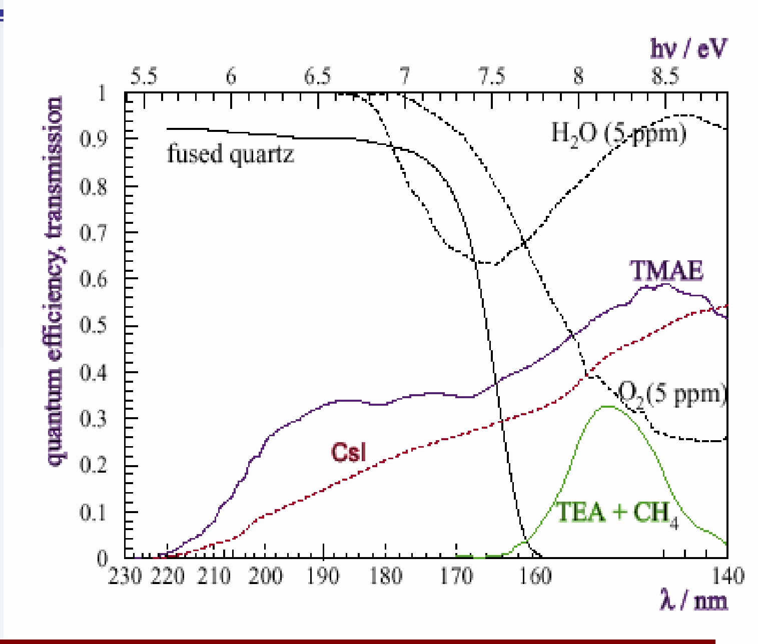

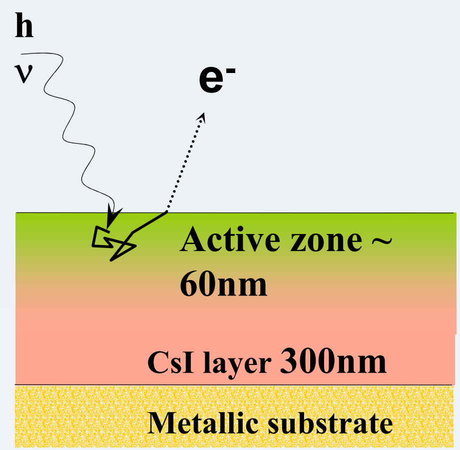

otosensor	E_{th}(eV)	vapour pression (torr)	l_{abs}(mm)	operational issues
TMAE	5.6	0.3	30	hazardous material, strong anode wire ageing
TEA	7.2	52	0.6	operation in the far UV: CaF_2+ultrapure gas mixture, high chromat.
CsI	5.6	-	$2\ 10^{-5\,(*)}$	moisture sensitive, long term ageing (?)

(*) electron escape length ~ O(10 nm)

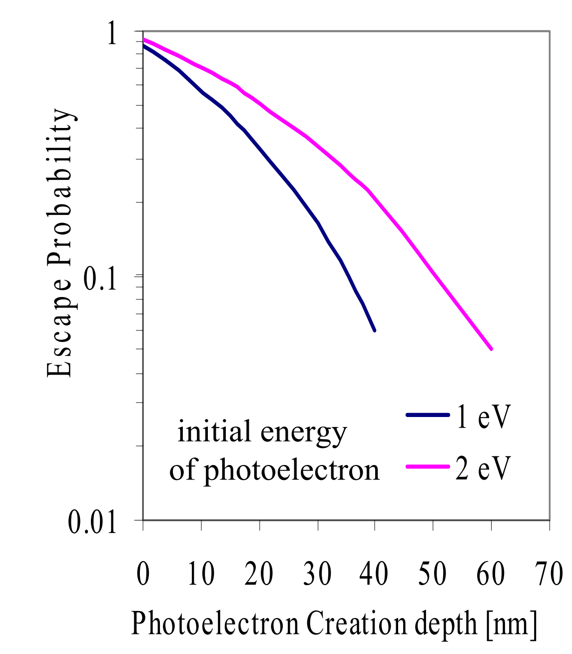

(A.Akkerman et Al., J.Appl.Phys.76(8)1994)

Gaseous photodetectors: intrinsic time resolution

hotosensitive vapours

tter created by drift time for different primary electrons:

$t \sim 3\sigma_t = 3 l_{ph}/v_d$

$_h$=photoabsorption length; v_d = electron drift velocity (O(100 μm/ns))

t = 10 ns → l_{ph}~ 0.3 mm (TEA at room temperature or TMAE at 100 ^{0}C)

sI

hotoelectrons are extracted isochronously →"FAST RICH DETECTORS"

eginning of 1990s: design of RICH counters for high luminosity B-factories operatin
: several MHz → digital measurement with fast (Δf=50 MHz) low noise current
mplifier → small charge induced on the cathode pads → small MWPC gap (~ 0.5 mm
: high gain 4-5$10^5$

ery high cathode gradient (8-10 kV/cm) → Unstable detector operation

reakthrough

D26 (F. Piuz et al., R&D for the development of large area CsI photocathodes, 1992)

ead-out electronics with long integration time (1.2 μs) → low gas gain (6-8 10^4)

ull detection efficiency & very stable detector operation attained

ow photon feedback → "open" geometry no blind electrodes

CsI Photocathodes

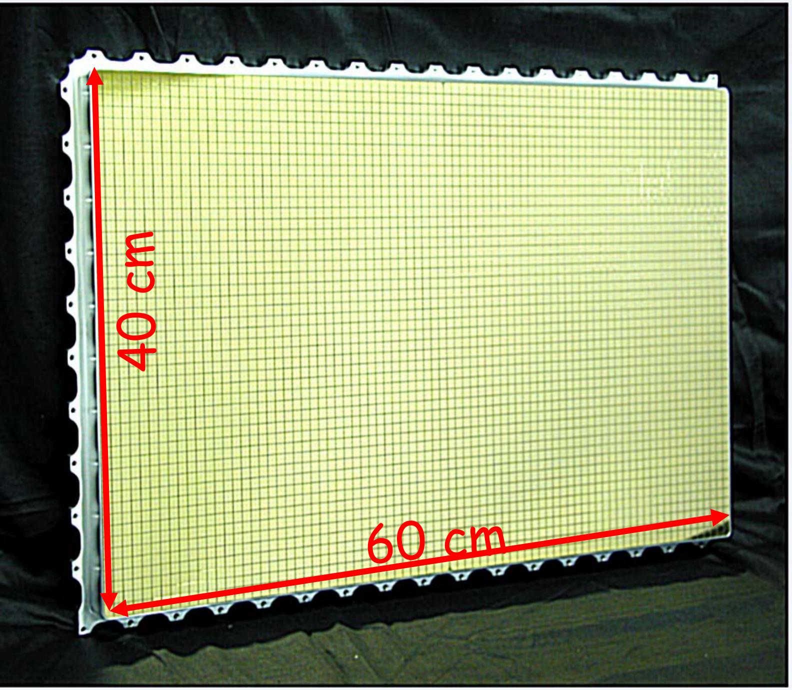

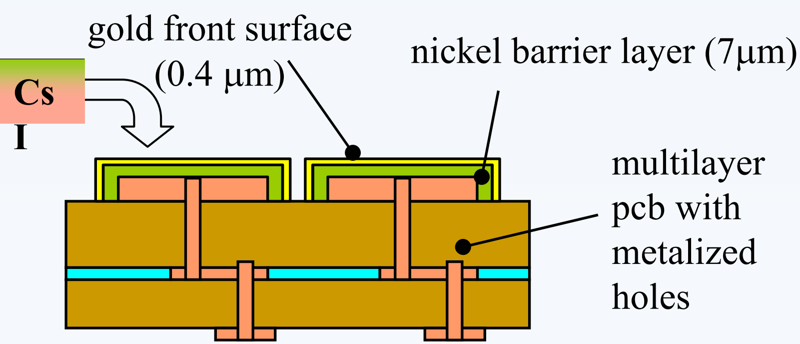

GROUND PLANE

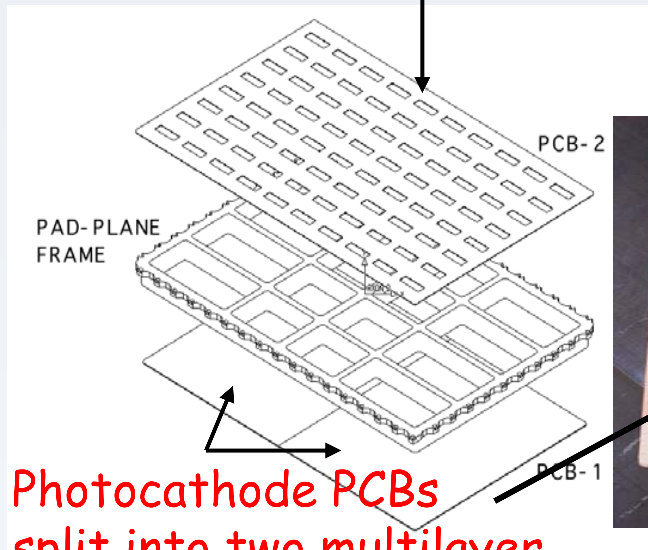

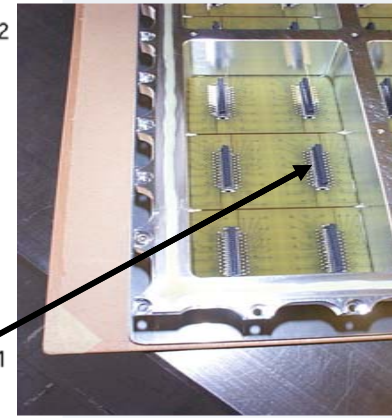

Photocathode PCBs
split into two multilayer
circuits (SMD connectors for FEE cards)

Identificazione di particelle

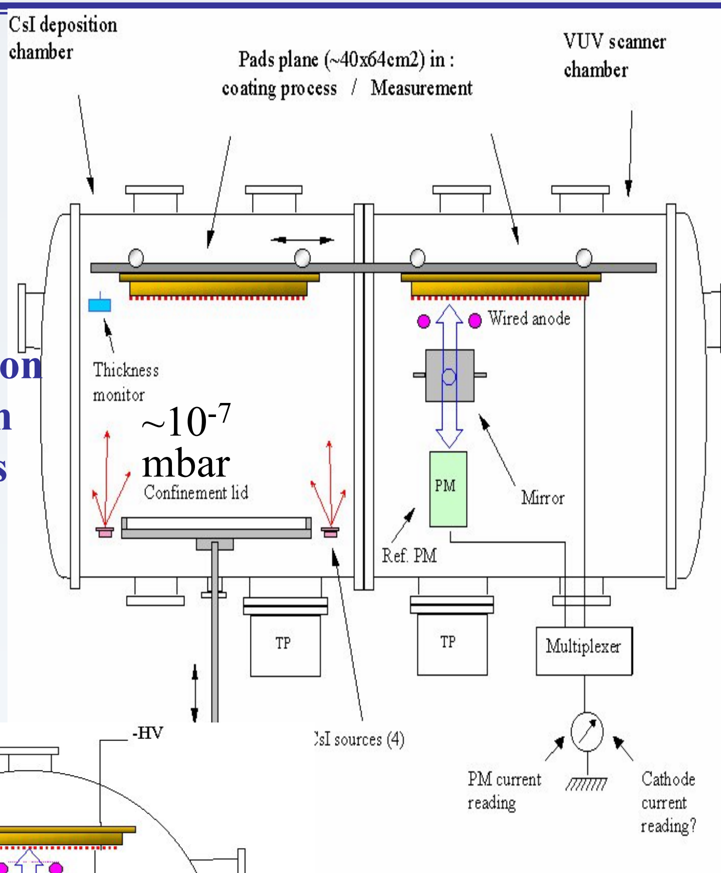

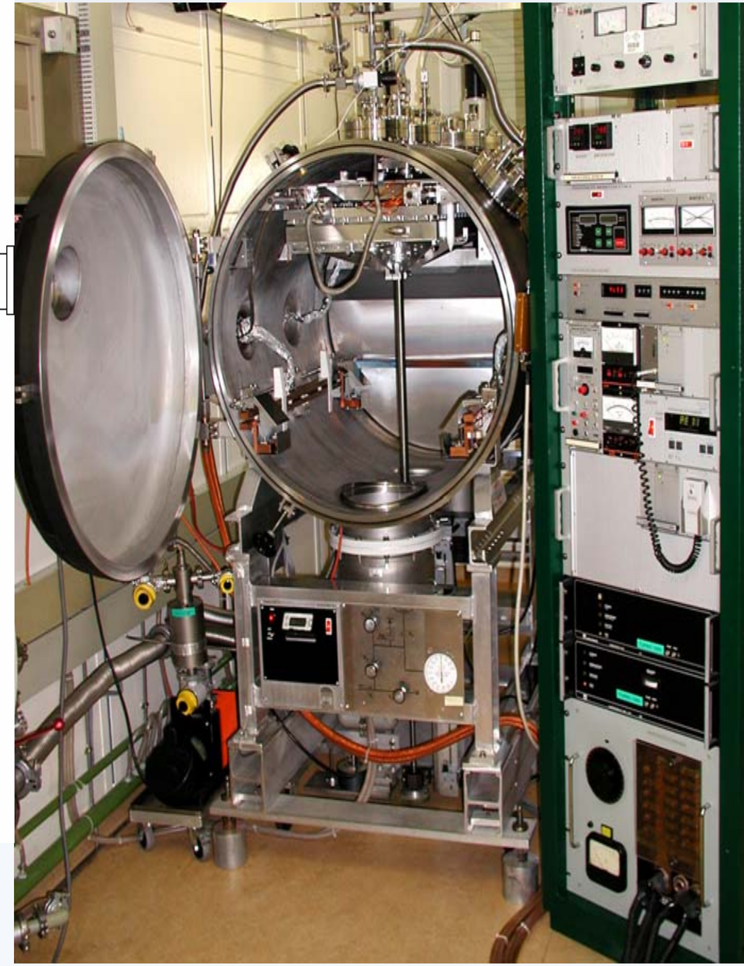

- low deposition rate (~1 nm/s)
  - → min. CsI dissociation
  - → little or no reaction with residual gases

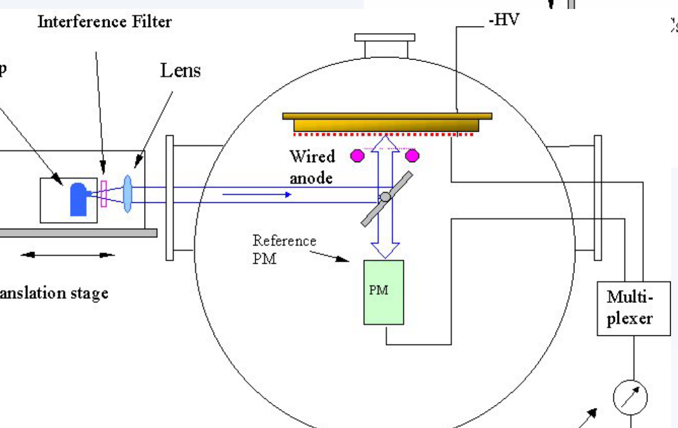

in situ QE evaluation under vacuum

- Thermal treatment during and after CsI deposition (~8 hrs at 60°C)
- In situ encapsulation under dry Argon before the implementation in the MWPC

E. Napi

CsI Quantum Efficiency

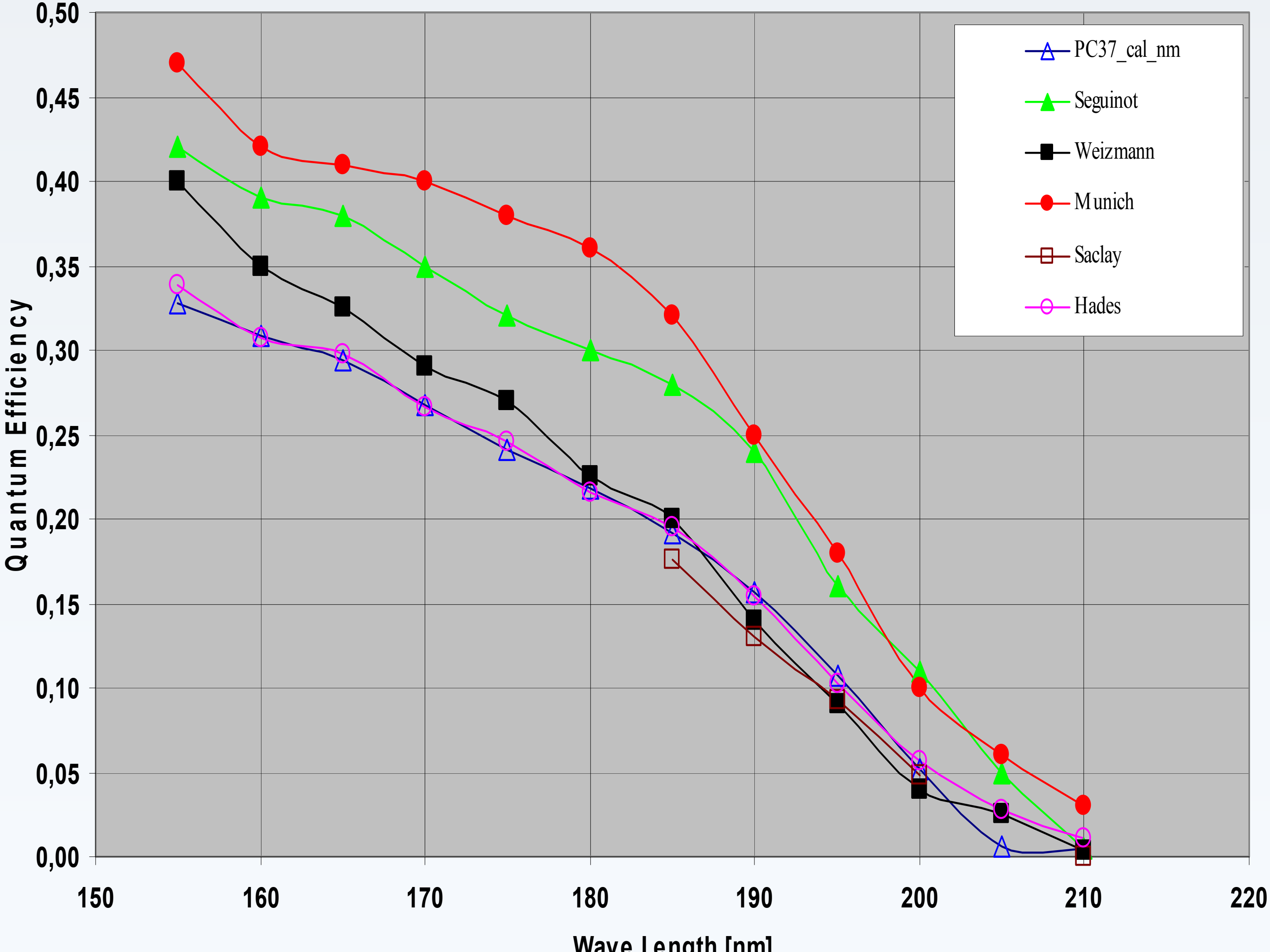

Experiments employing gaseous photon detector

Experiment	*π/K separation momentum range (GeV/c)*	*Max interaction rate (Hz)*	*Radiator (length)*	*Photon detector /surface(m^2)*	*Photocathode*	*Magnetic Field*
CLEO III	0.1-2.8	10^5	LiF (10 mm)	MWPC (CH_4) / 14	TEA	1.5 T
HADES-GSI	0.1-1.5 (hadron blind)	10^6	C_4F_{10} (0.5 m)	MWPC (CH_4) / 1.4	CsI	NO
ALICE-LHC	0.8 – 3	10^4	C_6F_{14} (10 mm)	MWPC (CH_4) / 12	CsI	0.5 T
TJNAF - Hall A	0.8 - 3	10^6	C_6F_{14} (10 mm)	MWPC (CH_4) / 2	CsI	NO
COMPASS-SPS	3 -120	10^6	C_4F_{10} (3 m) / N_2+C_2F_6 (8 m)	MWPC (CH_4) / 8 (RICH-1)	CsI (RICH-1)	NO

Note:

- large area coverage (up to several m^2)
- operation in magnetic field

E. Napi

From UV to Visible Light Imaging

Recent trend in RICH technique: shift the detector design from UV to visible

Driven by:

- Ever increasing acquisition rate of future experiments
- Availability of multianode PMTs and hybrid devices
- Exploitation of aerogel as radiator medium

Multi-anode Photomultipliers MaPMTs (HERA-B,AMS)

Quantacon-like PMTs (DIRC,SELEX,HERMES)

Hybrid Photo Diodes HBDs (LHCb, BTeV)

Cherenkov Light from Aerogel

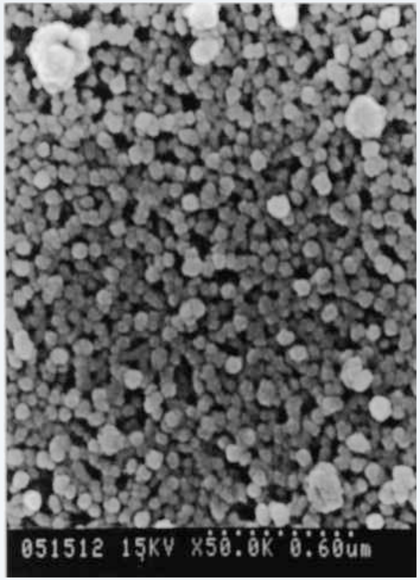

AEROGEL: "A little bit of almost nothing"
(the lightest solid, ρ: 3-350 mg/cc)

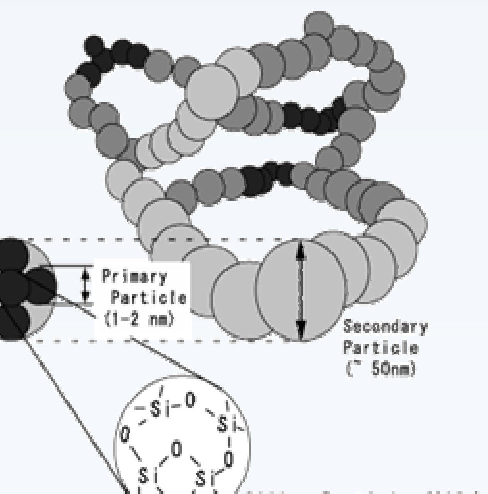

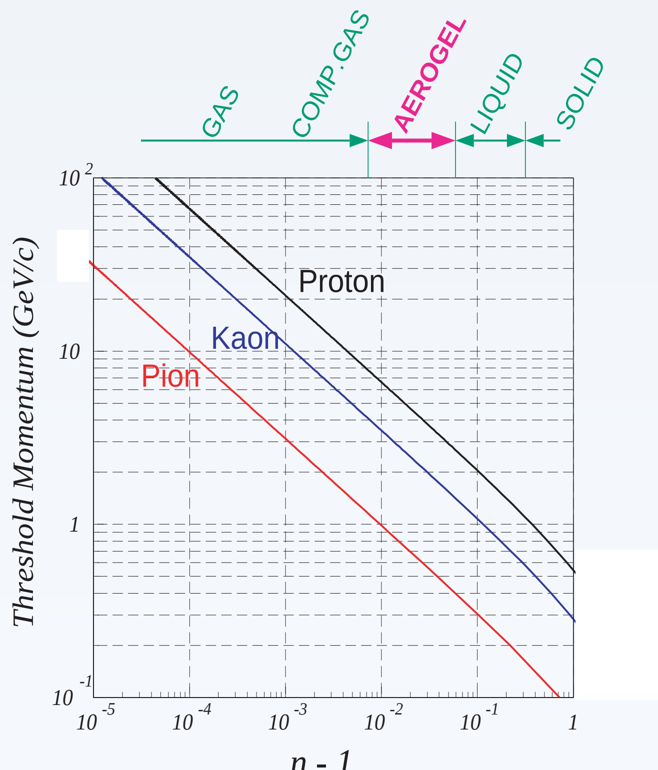

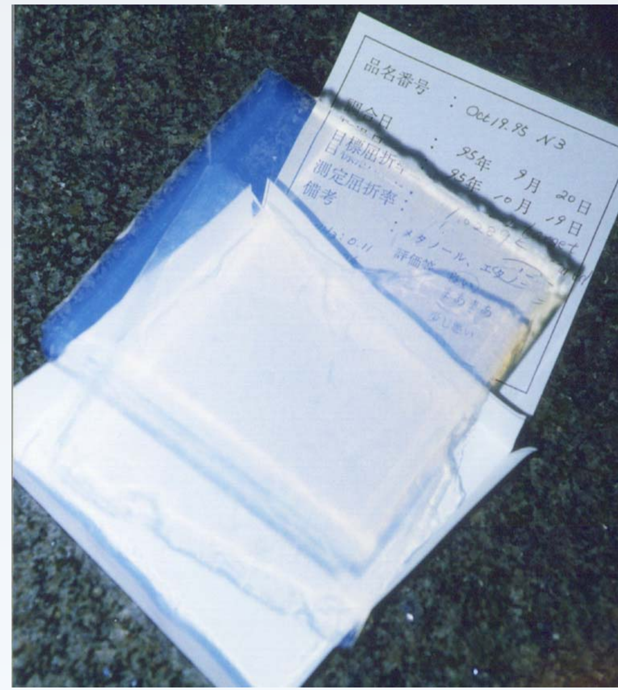

production of hydrofobic aerogel of outstanding quality driven by BELLE

Holy Grail

erogel is used in more than 800 applications

smic dust or meteoroid fragments
softly captured
(impact damage minimized)

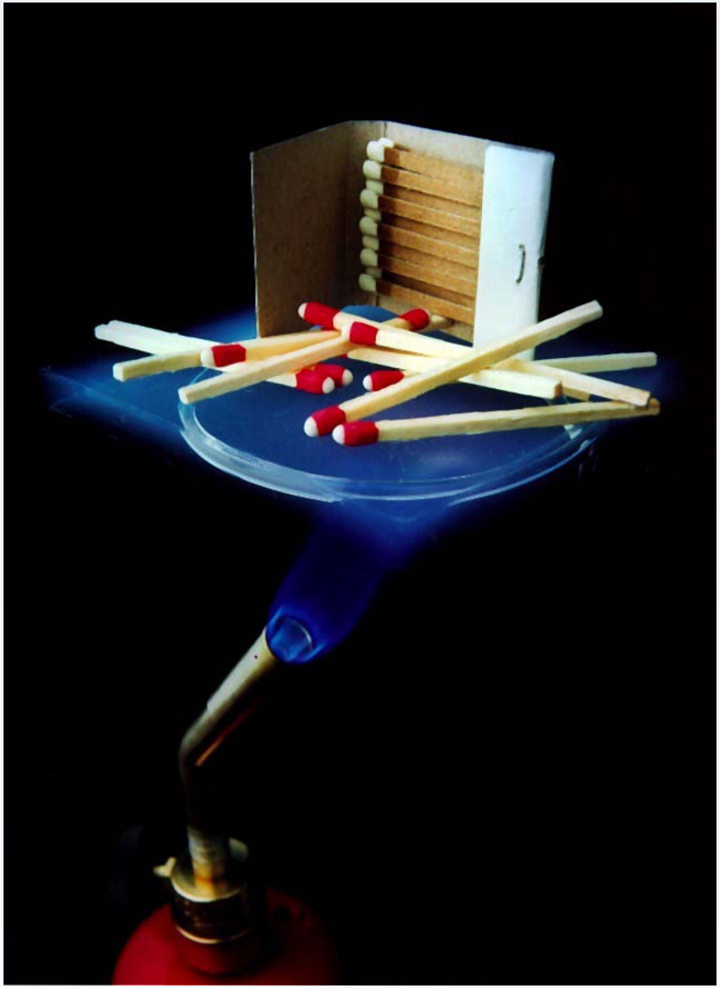

thermal conductivity ~ 0.017 W/m

Identificazione di particelle

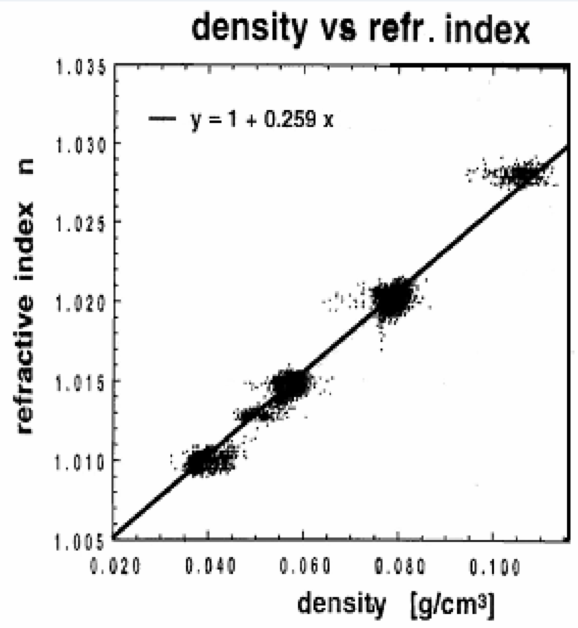

$n=1+0.26*\rho$

Radiator	Refractive index (7 eV)	π threshold momentum (GeV/c)	K threshold momentum (GeV/c)	p threshold momentum (GeV/c)
C_6F_{14}	1.28	0.18	0.62	1.18
Aerogel	1.03	0.6	2	3.8
C_4F_{10}	1.0015	2.5	8.9	17

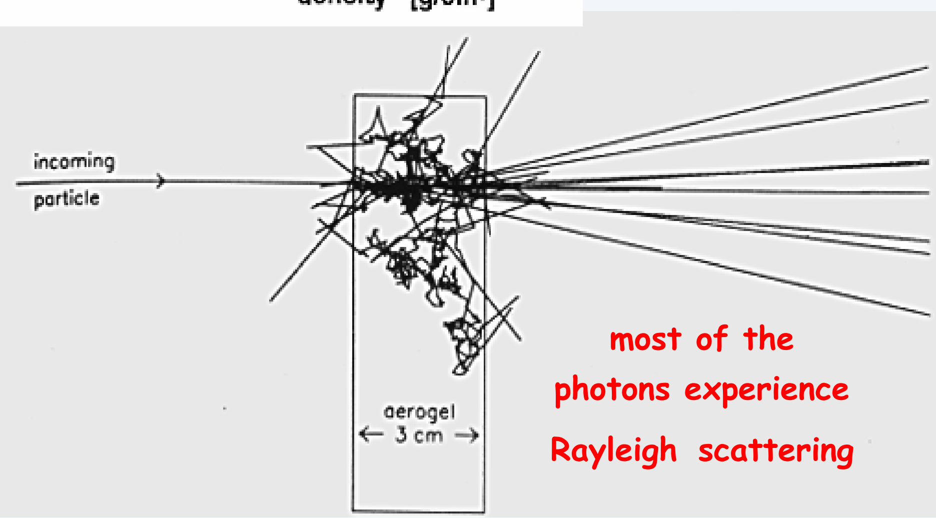

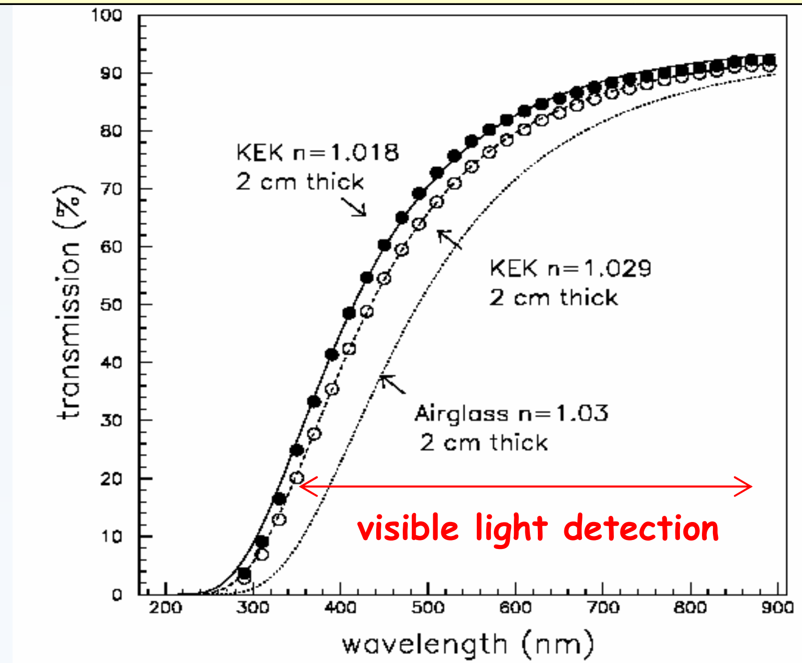

Issues in Visible Light Imaging

Advantages

⇒ improved performance (large N_0, small chromatic aberration, rate capability)

⇒ wider range of materials for detector construction

⇒ easy to operate

Disadvantages:

⇒ large dead area due to small filling factor (packing density)

⇒ most of photon detectors do not work in magnetic field

⇒ high cost per channel (limited coverage applications)

HERMES

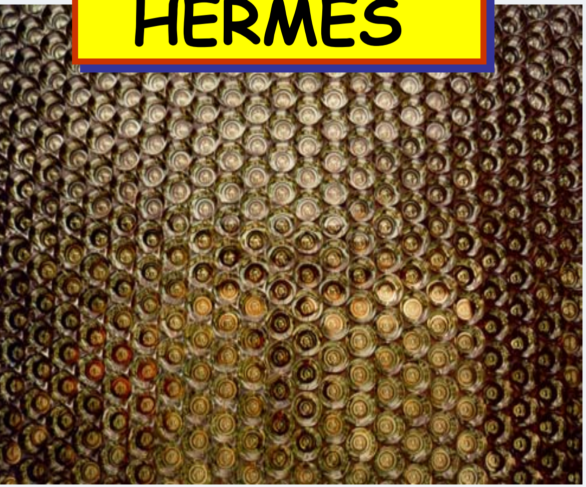

3870 PMTs, Philips XP1911/UV, Ø 3/4” + light funnels

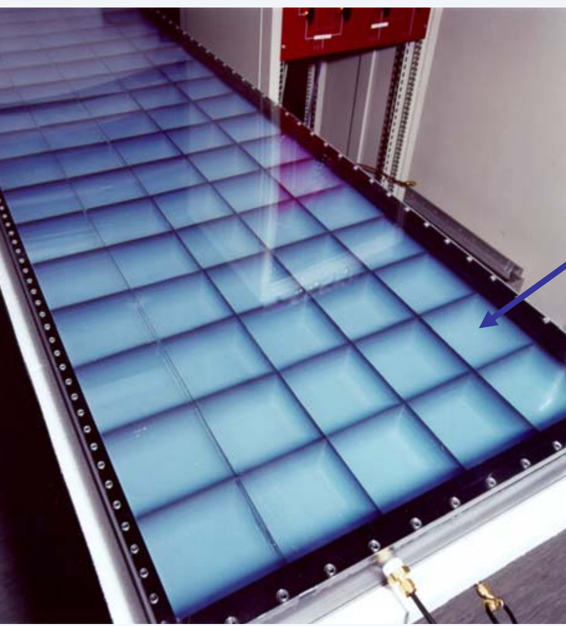

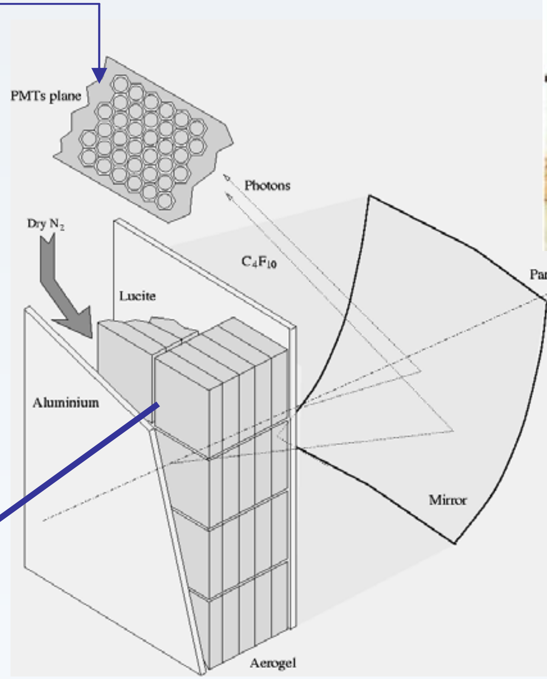

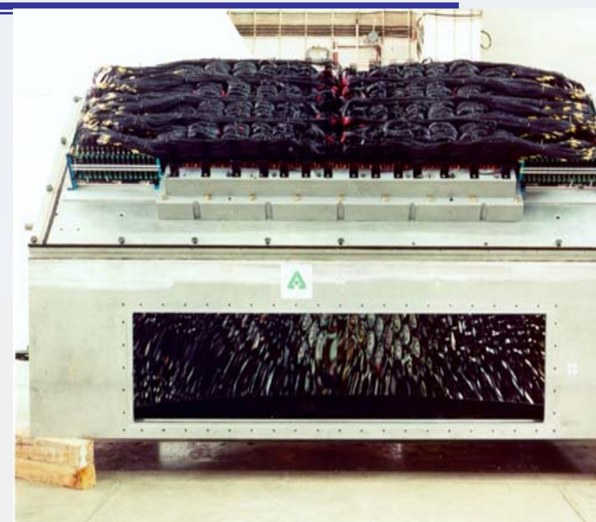

Online Event Display

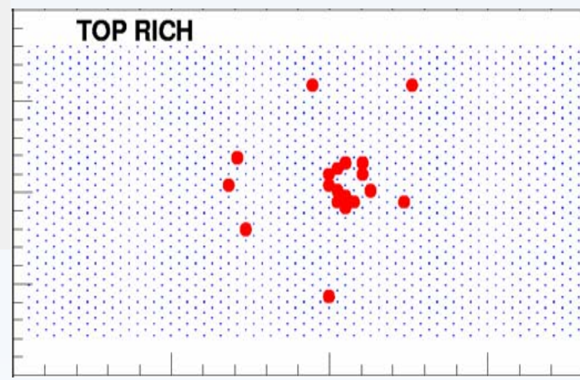

$<N_{p.e.}$ (aerogel)$>$ = 8

$<N_{p.e.}$ $(C_4F_{10})>$ = 12

RICH Detectors in LHCb

Forward single-arm spectrometer

Observe CP violation in decays of B mesons produced in p-p collisions at E_{cm}= 14 TeV

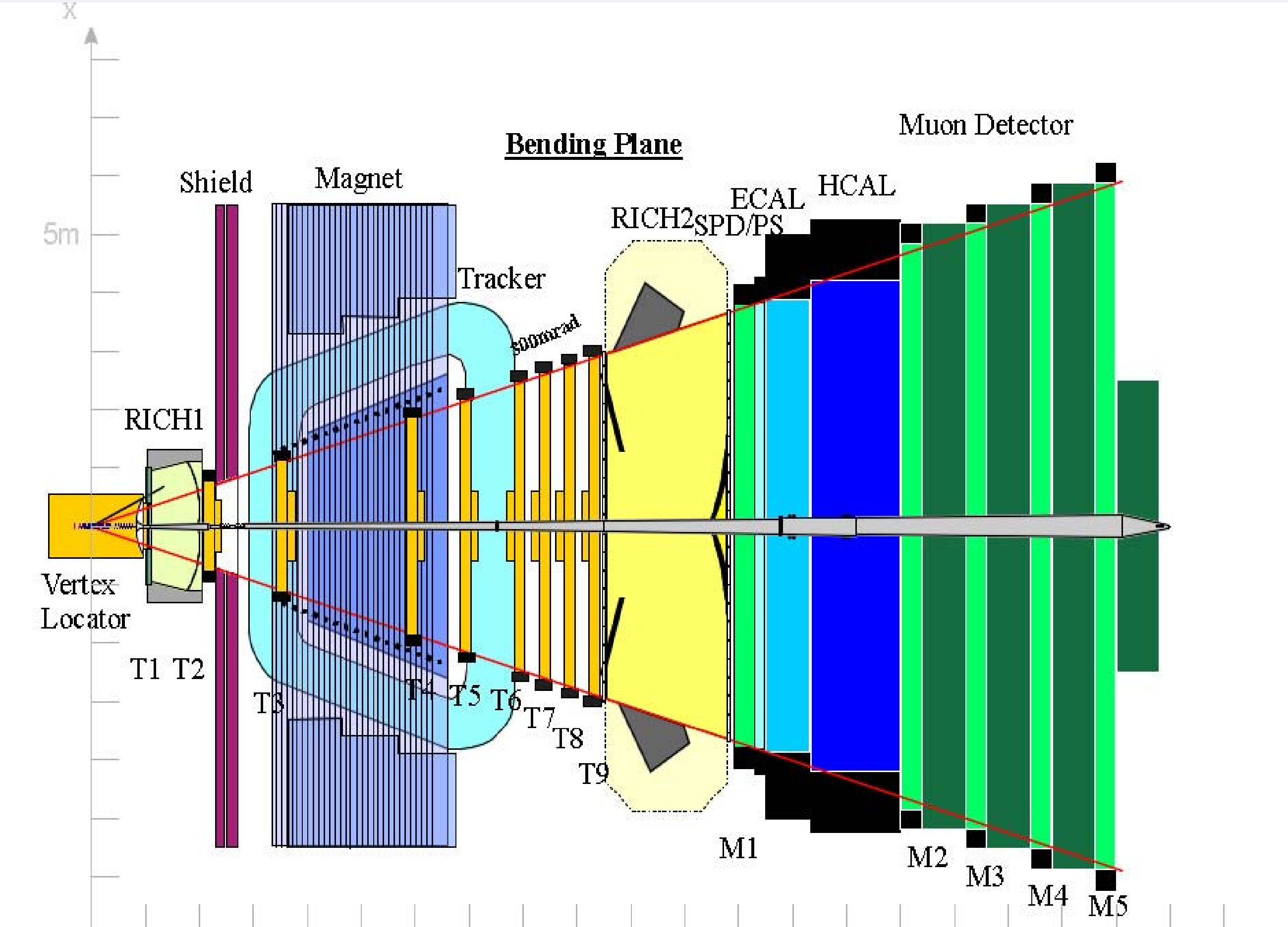

RICH1 and RICH2 detectors

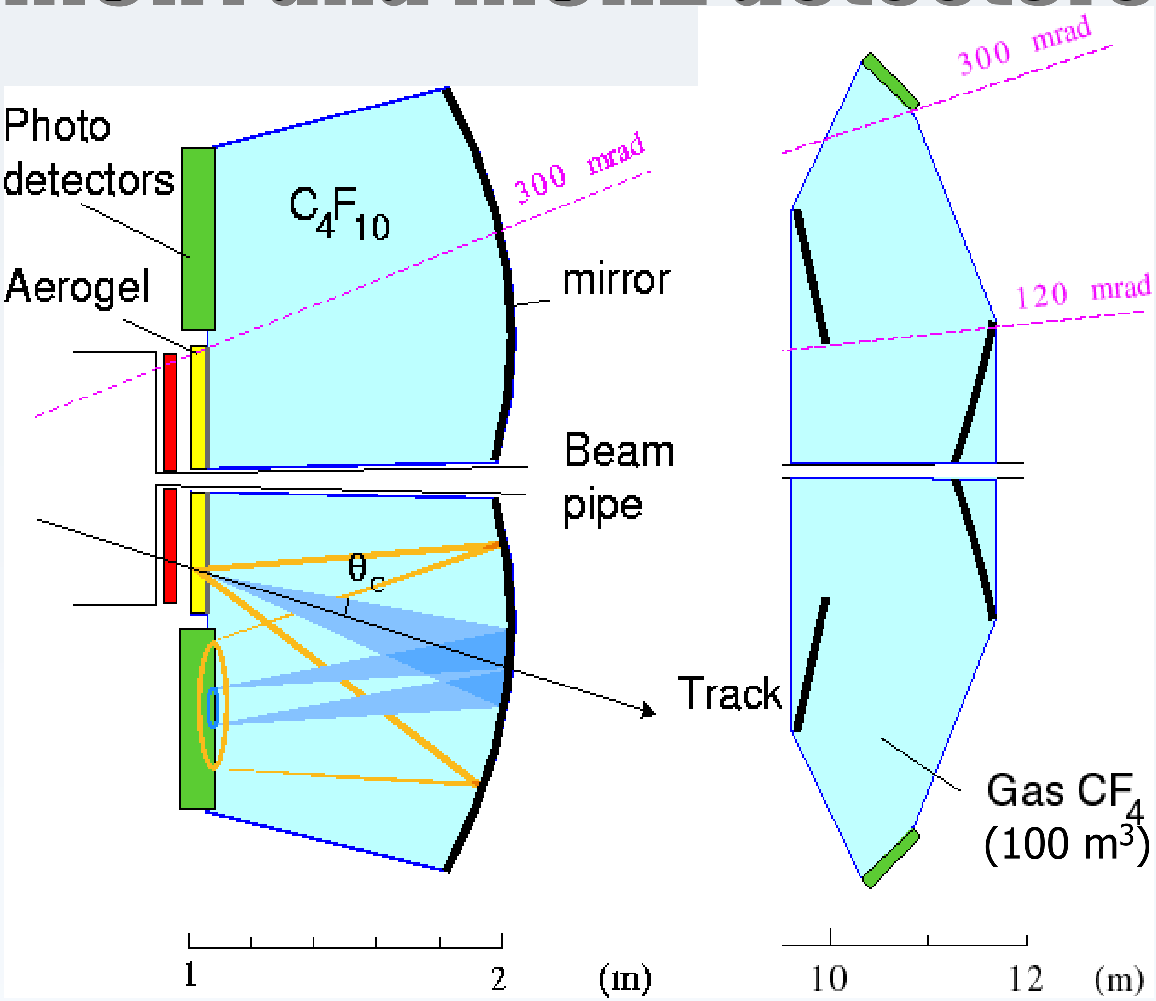

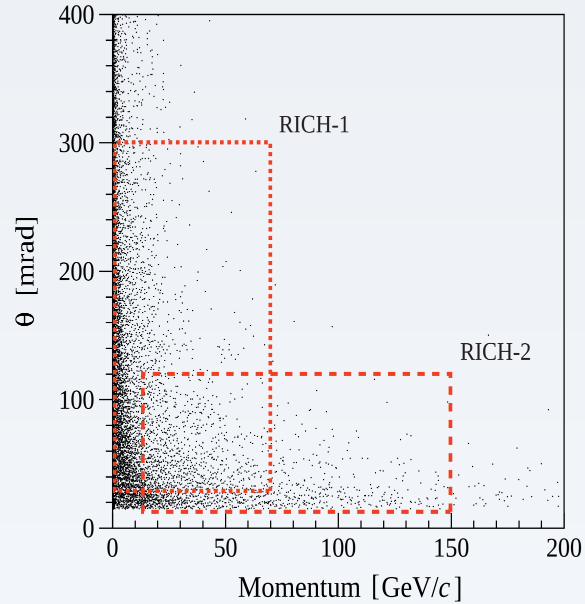

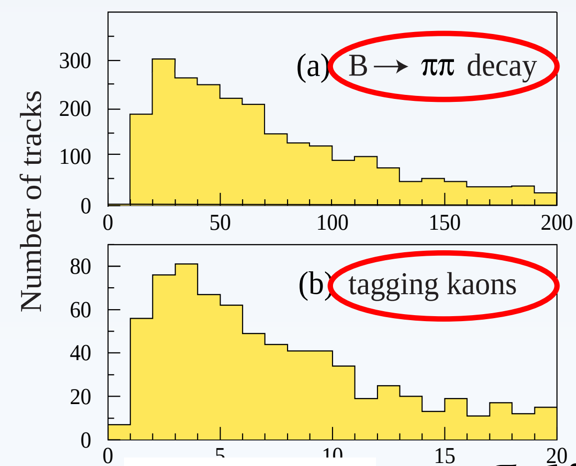

Momentum (GeV/c)

Acceptance: **300 mrad RICH1**

120 mrad RICH2

E. Napi

Radiators

Three Cherenkov radiators are used, to cover the full momentum range:

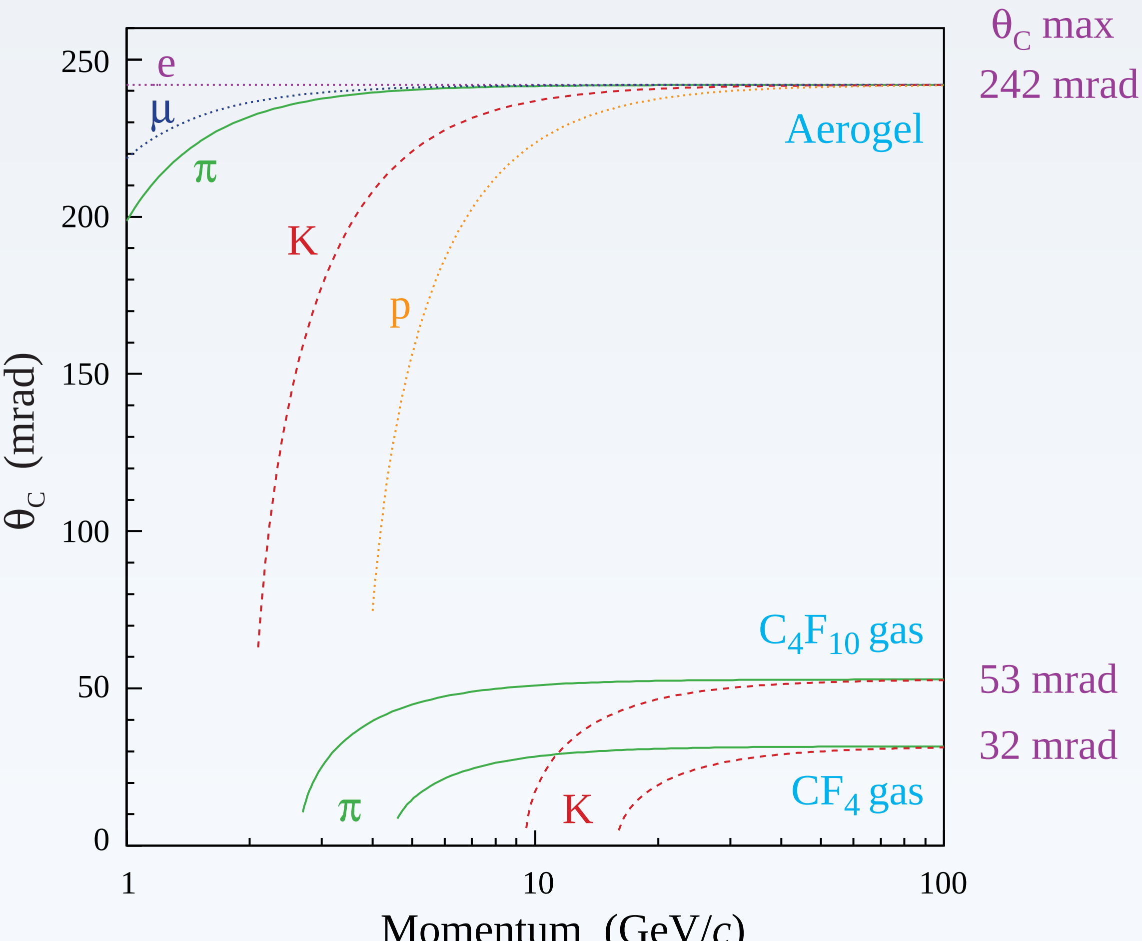

RICH1

Aerogel (n = 1.03)

1-10GeV/c

C_4F_{10} (n = 1.0014)

10-60GeV/c

RICH2

CF_4 (n = 1.0005)

17-100GeV/c

Photon Detector

~ 3 m^2 area have to be equipped with photodetectors providing:

- Single Photon Sensitivity (200 - 600nm)
- 2.5 x 2.5 mm^2 granularity
- Fast readout (40 MHz)
- Active-area fraction > 70%

Hybrid Photo Diodes (HPD)

168 HPDs RICH1
262 HPDs RICH2
} 340 K channels

Hybrid Photon Detector

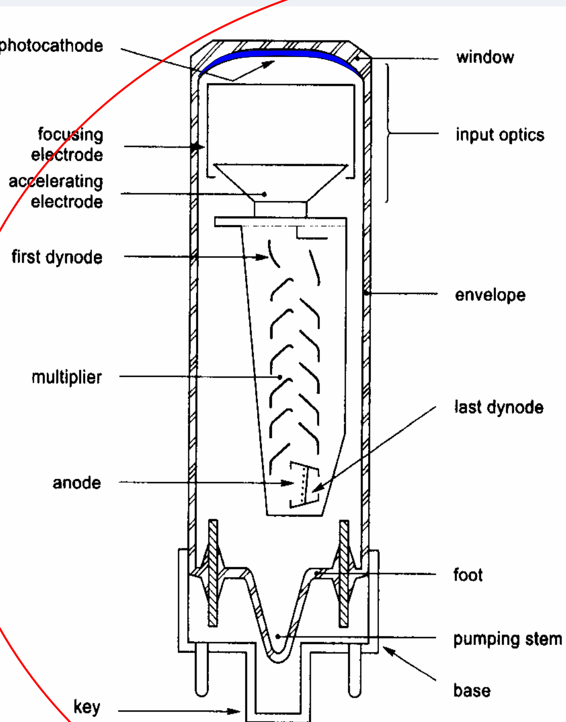

Photomultiplier

+

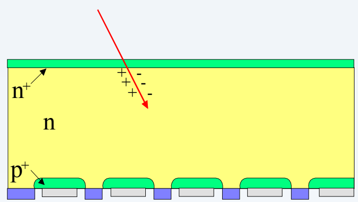

Silicon Sensor

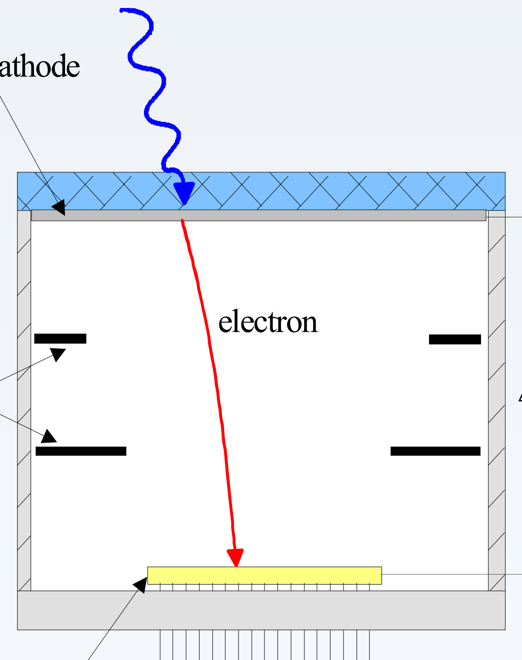

Hybrid Photo Diod

Identificazione di particelle

HPD Features

Gain is achieved in a single dissipative step

ΔV=20 kV Ee = 20 keV
in silicon: 3.6 eV ≈ 1 e/h pair -> 20 keV ≈ 5000 e/h
G~5000

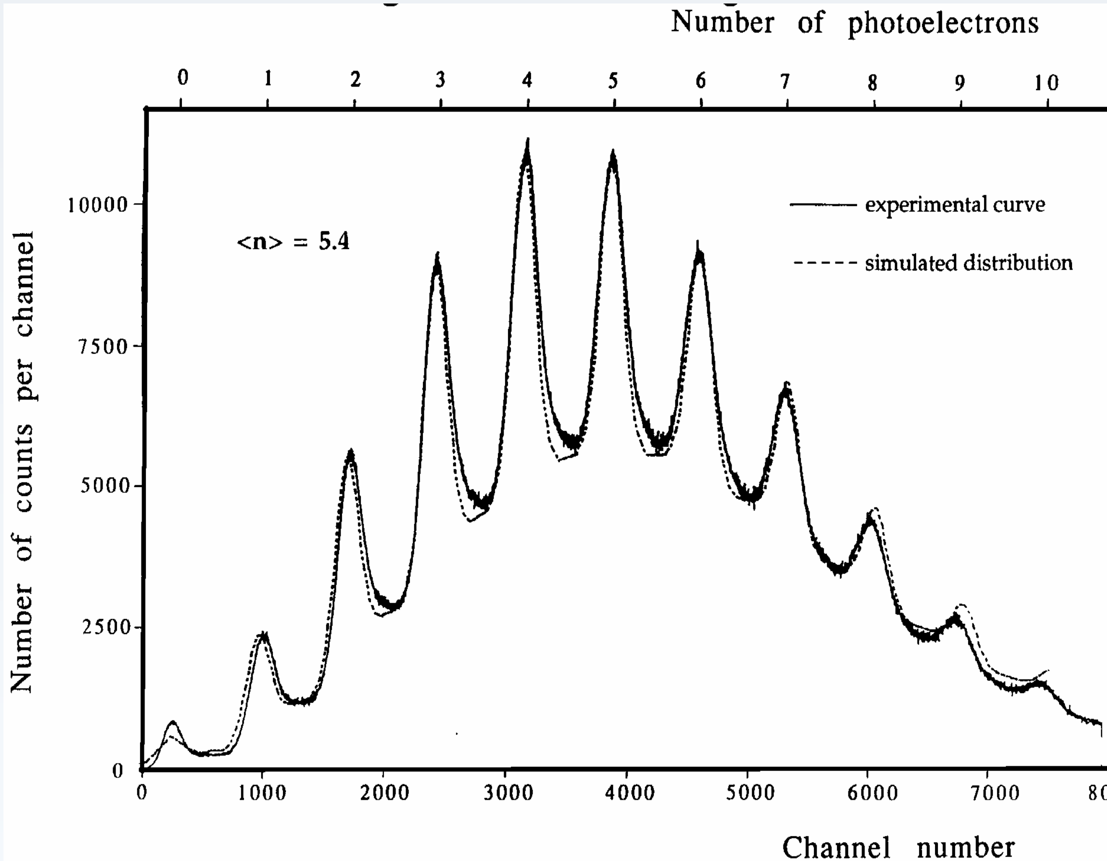

Advantages

Excellent signal definition
Allows for photon counting
Free choice of pixel segmentation (50 μm - 10 mm)
Uniform sensitivity and gain
no dead zones between pixels

Drawbacks

- Low gain (3000 - 8000) → low noise electronics requir
- Sensitivity to magnetic fields

Identificazione di particelle

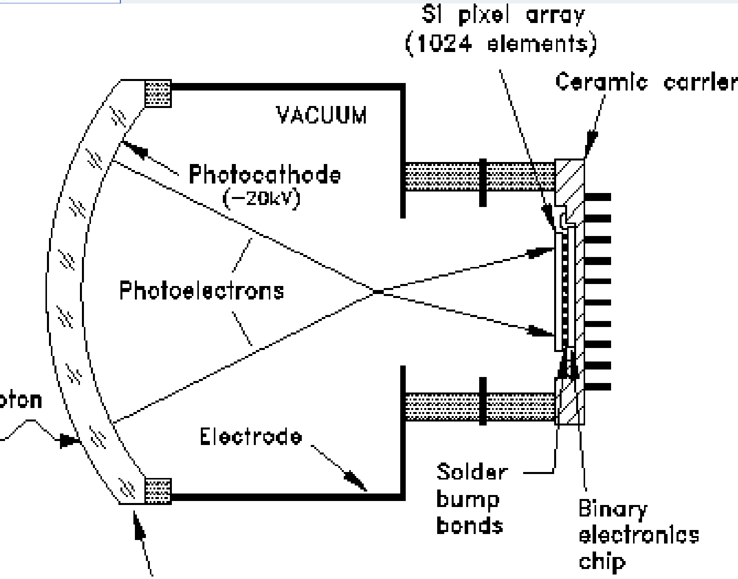

83 mm diameter
75 mm photocathode diameter

82% active area

- Quartz window
- S20 photo cathode $\int QE\, dE = 0.77$ eV
- 1024 (320 x 32) Si pixel array: 500 μm x 50 μm
- Cross-focusing optics
  - demagnification ~ 5 (pixel size at photocathode 2.5 x 2.5 mm^2)
  - 50 μm point-spread function
  - 20 kV operating voltage **5000 e** signal at Si anode
- Encapsulated binary electronics
- Tube, encapsulation: DEP (NL)
- Silicon Pixel sensor bump bonded to readout chip

Flip-chip technique

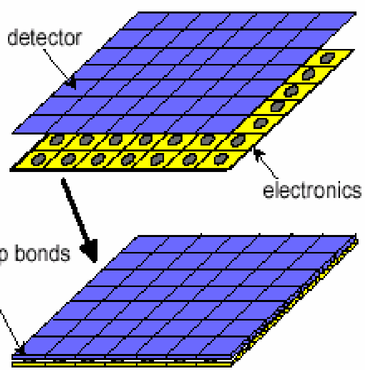

RD 19, E. Heijne et al., NIM A 384 (1994) 399

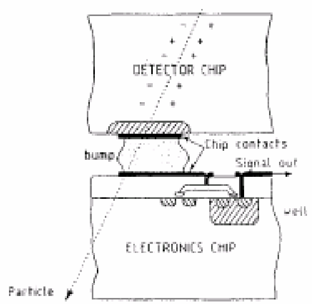

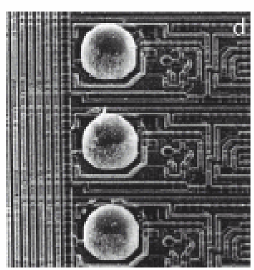

LHCb Pixel-HPD

LHCb PID Performance

Most relevant parameters for physics analysis are K selection efficiency and $\pi \rightarrow$ K misidentification rate

$\langle\varepsilon_{K\rightarrow K}\rangle = 88\ \%\quad (2\text{–}100\ \text{GeV}/c)$

$\langle\varepsilon_{\pi\rightarrow K}\rangle = 2.7\ \%$

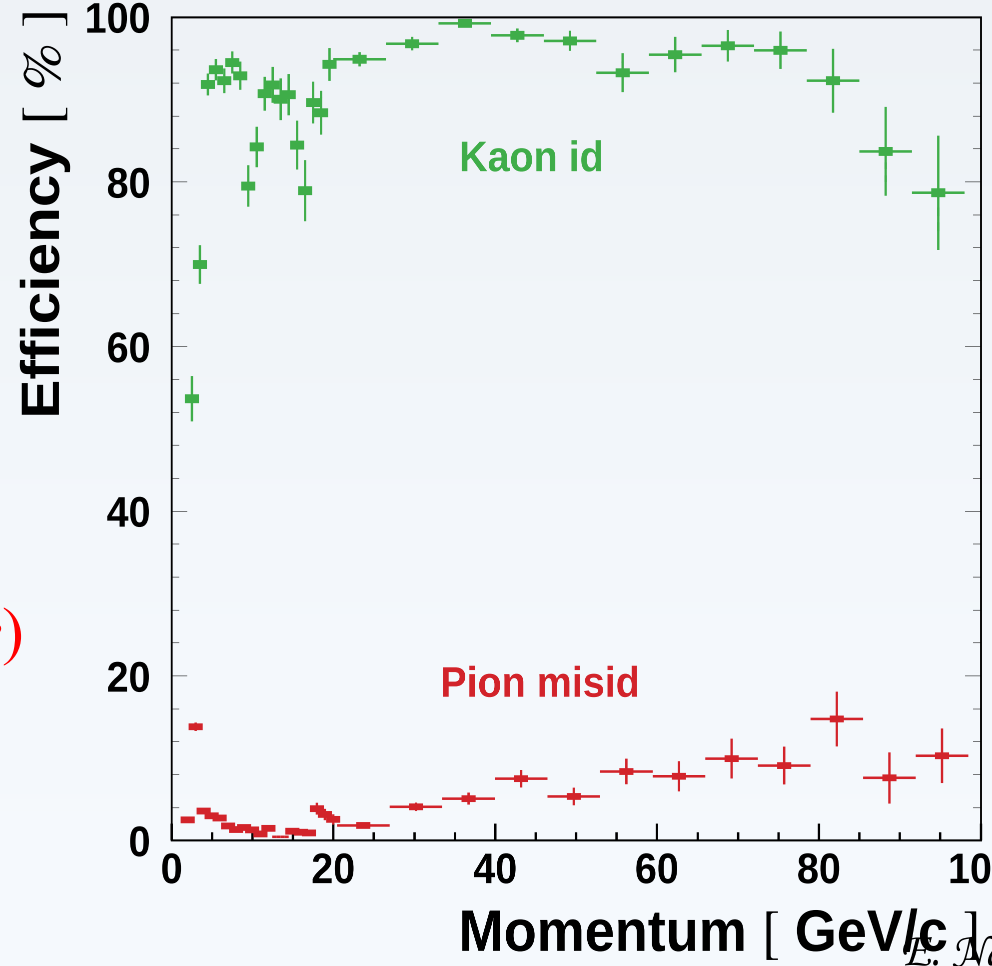

Transition Radiation

Transition Radiation (TR) occurs when a particle traverses a medium with a discontinuous refractive index, i.e. the boundary of two media with different dielectric properties.

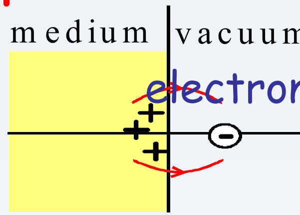

TR is the result of the fast rearrangement of the particle e.m. field when displacing from one medium to the other characterized by another phase velocity.

A kind of dipole radiation (charged particle and its mirror image)

Analogy with flying fishes: the light that reaches the observer's eyes experiences the different refractive indices of water and air thus featuring an <u>"apparent"</u> acceleration of the fish

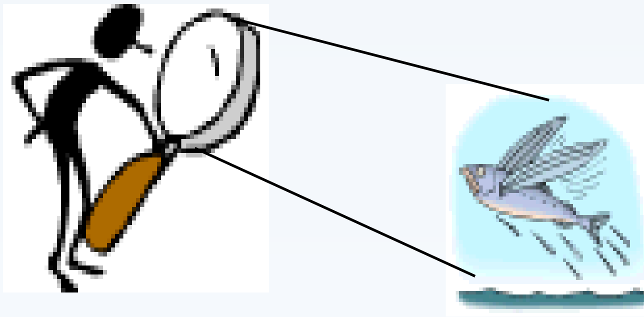

Transition Radiation Application to PID

The phenomenon was first predicted by two Russian physicists, Ginsburg and Frank, in 1945 (J. Phys.9(1945)353)

More than 20 years later, the first TR detector was exploited successfully in a HEP experiment at the CERN-ISR thanks to Garibyan who found in 1958 that ultra relativistic particles (γ>>1) emit TR in the X-band and that the radiated energy is proportional to the particle's Lorentz factor γ (i.e. the particle's energy).

Since the other particle identification methods (energy loss by ionization, ToF and Cherenkov radiation) depend on the particle velocity, thereby representing only moderate identification possibilities for ultra relativistic particles (β -> 1), the γ-dependent effect of TR is extremely valuable for PID at very high energies.

Unitary Description of the Radiative Processes

A photon in a medium has to follow the dispersion equation:

$$\omega = 2\pi\nu = 2\pi\frac{c/n}{\lambda} = k\frac{c}{n} \qquad \omega^2 - \frac{k^2c^2}{\varepsilon} = 0 \qquad \varepsilon = n^2$$

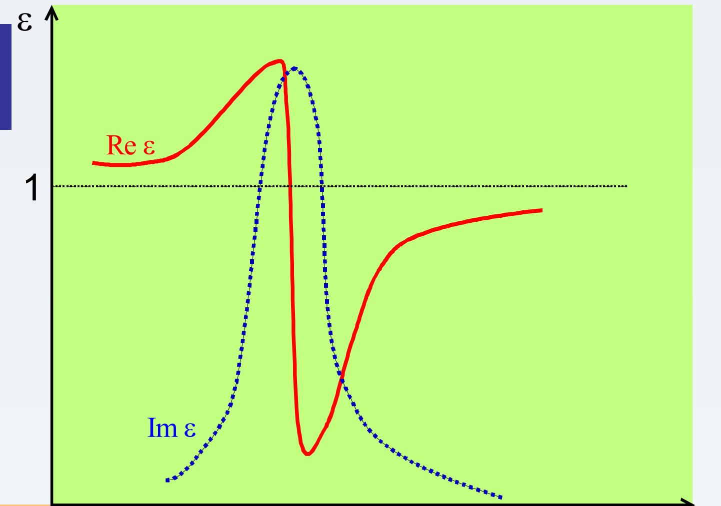

regime:	optical	absorptive	X-ray
effect:	Cherenkov radiation	ionisation	transition radiation

ε=Re(ε)+i Im(ε)
Im(ε): photon absorption in the medium
ε=ε(ω)
ε describes the way the interaction of photons with atoms of the medium modifies the phase velocity

- Optical band: transparent medium, ε=Re(ε) >1, $n \sim 1 - \frac{\omega_p^2}{2\omega^2}$
  ⇒ emission of real photons with u=c/n: Cherenkov radiation
- Absorptive (or resonant) band: ε=Re(ε)+ iIm(ε), virtual photo and short range, the medium is not transparent
  ⇒ dE/dx in the medium
- X-band: ε < 1
  ⇒ emission of X-ray transition radiation

Transition Radiation Spectrum

$$\frac{d^2W}{d\omega d\theta} = \frac{2\alpha\hbar\theta^3}{\pi}\left(\frac{1}{1/\gamma^2+\theta^2+\omega_1^2/\omega^2} - \frac{1}{1/\gamma^2+\theta^2+\omega_2^2/\omega^2}\right)^2$$

$$\frac{dW}{d\omega} = \frac{\alpha\hbar}{\pi}\left[\left(\frac{\omega_1^2+\omega_2^2+2\omega^2/\gamma^2}{\omega_1^2-\omega_2^2}\right)\times\ln\left(\frac{1/\gamma^2+\omega_1^2/\omega^2}{1/\gamma^2+\omega_2^2/\omega^2}\right)-2\right]$$

Energy loss by the TR increases with γ linearly

$$W = \frac{\alpha\hbar}{\pi}\frac{(\omega_1^2-\omega_2^2)}{\omega_1+\omega_2}\gamma$$

ω_1 and ω_2 are Plasma frequencies of two media

$$\hbar\omega_p = \sqrt{4\pi N_e r_e^3}\, m_e c^2/\alpha$$

~20eV for styrene.

Transition Radiation properties

- Radiated energy / boundary to vacuum

$$W = \frac{1}{3}\alpha\hbar\omega_p\gamma \qquad \boxed{W \propto \gamma} \longrightarrow \text{Identification of } e^{\pm}$$

$$\omega_p = \sqrt{\frac{N_e e^2}{\varepsilon_0 m_e}} \quad \left(\begin{matrix}\text{plasma}\\ \text{frequency}\end{matrix}\right) \quad \hbar\omega_p \approx 20\text{eV (plastic radiators)}$$

- X-rays are emitted with a sharp maximum at small angle $\theta \propto 1/\gamma$ $\rightarrow$ TR stay close to track

- Number of emitted photons / boundary is small

$$N_{ph} \approx \frac{W}{\hbar\omega} \propto \alpha \approx \frac{1}{137}$$

Need many transitions $\rightarrow$ build a stack of many (>100) thin foils with gas gaps

Identificazione di particelle

Ideal radiator: material with high density of electrons (high ω_p) and low Z (small X-ray absorption $\propto Z^5$)

	DENSITY (g cm^{-3})	PLASMA FREQUENCY (eV)	COEFFICIENT OF LINEAR ABSORPTION @10 KeV (cm^{-1})	X_0 (cm)
Lithium	0.534	13.8	7.1 10^{-2}	14.8
Berillium	1.84	26.1	7.2 10^{-1}	34.7
Aluminium	2.70	32.8	71.4	8.9
Polyethylene	0.925	20.9	1.79	49
MYLAR	1.38	24.4	8.07	28.7
Air	2.2 10^{-3}	0.7	9.1 10^{-2}	3087 0

For practical reasons (availability, price, safety) mainly stacks of CH_2 foils are used. Li foils not significantly more performing. Also various hydrocarbon foam and fiber materials have been used. TR yield in foams are smaller than in regular stacks due to large dispersion of mean foil thickness and pore size.

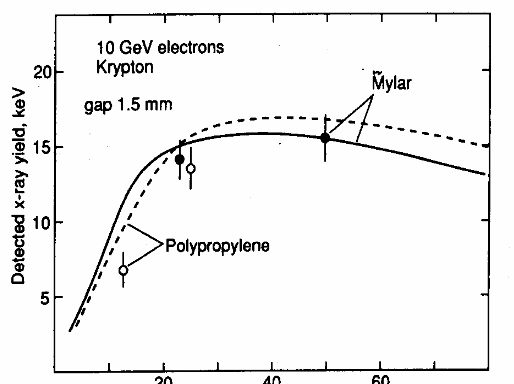

Variation of TR yield with foil thickness

Part of the TR will be re-absorbed. This limits the effective number of foils even for $N_f=\infty$

Identificazione di particelle

Simulated emission spectrum of a CH_2 foil stack → Detector should be sensitive for $3 \leq E_\gamma \leq 20$ keV.

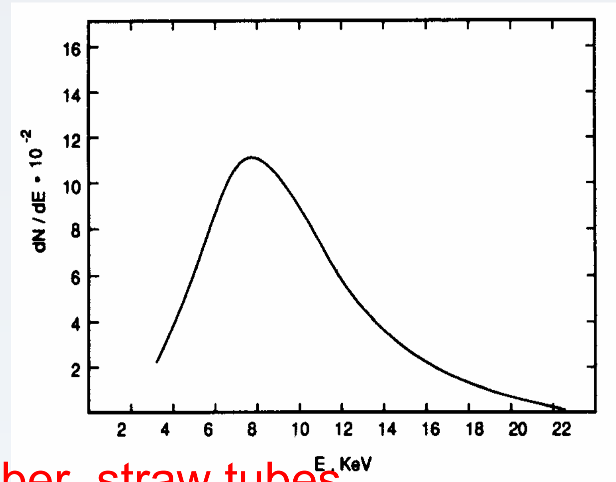

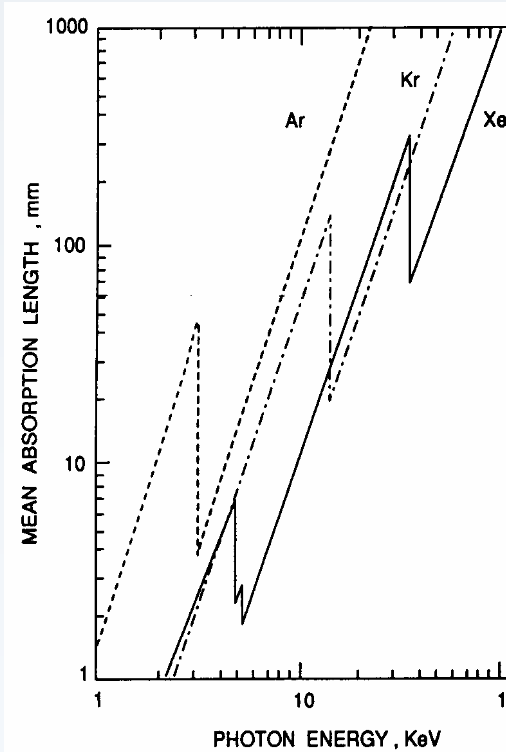

ainly used: Gaseous detectors.
MWPC, drift chamber, straw tubes…

etector gas: $\sigma_{\text{photo effect}} \propto Z^5$ → gas with high Z required (Xe, Kr
r Ar)

ignal: TR+dE/dx (TR emitted at $1/\gamma$)

Absorbed flux fraction

$$\alpha = \left(1 - e^{-l/\lambda}\right)$$

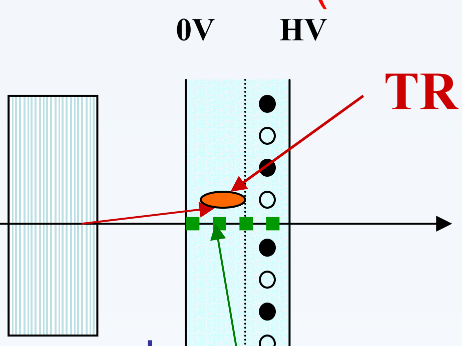

dE/dx

ackground:
δ electrons

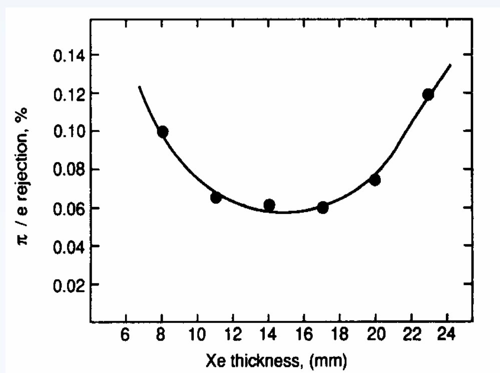

Chamber thickness:
compromise between γ absorption and ionization background from charged particles. Typically 10 -15 mm

E. Napi

Identificazione di particelle

Issue: **need to separate dE/dx signals and TR x-ray signals**

Two possible readout methods:

- Charge (Q-) method. Integrate all collected charge from dE/dx + TR (above a certain threshold). Apply cut to suppress particles with dE/dx only. Limited by Landau tails of dE/dx.
- Cluster counting. Identify individual ionization clusters. Count clusters above a certain threshold (from high energy γ's). Lower background because $N_{cluster}$ is Poisson distributed. But requires fast electronics and special chamber geometry

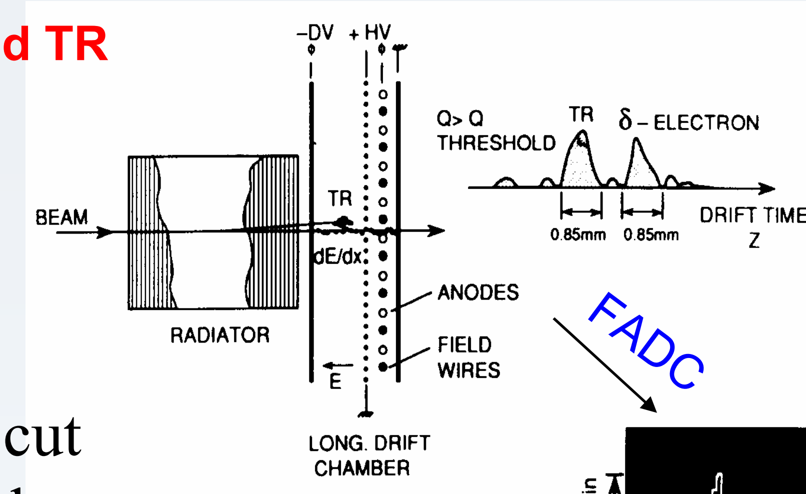

FADC

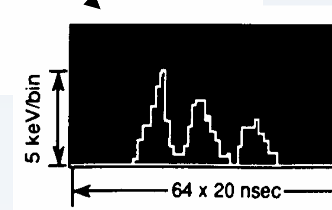

T. R. Detector read-out

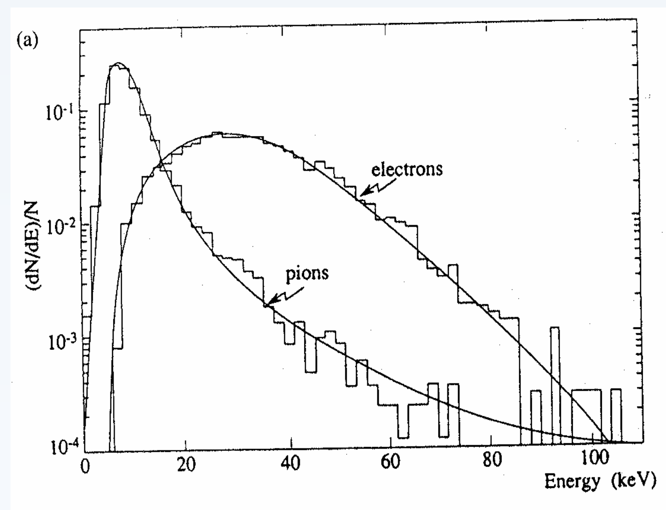

Transition Radiation Detectors in ATLA

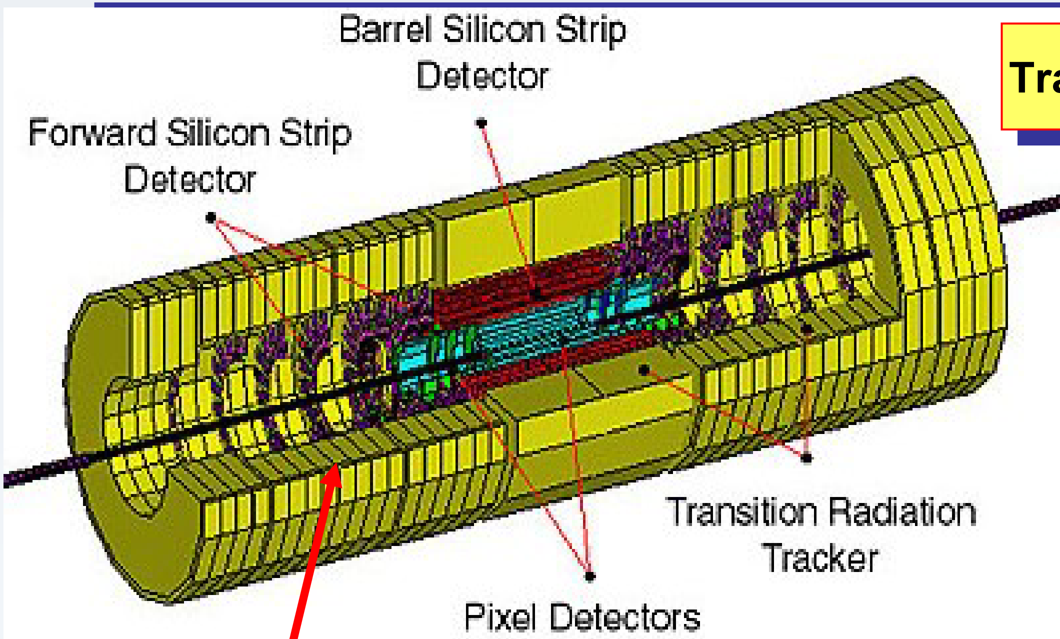

Straws (4 mm diameter)
Regular radiator: 15 μm polyethylene foils with 200 μm spacing

$\varepsilon_\pi \sim 10^{-3}$-$10^{-2}$ @ $\varepsilon_e \sim 90\%$

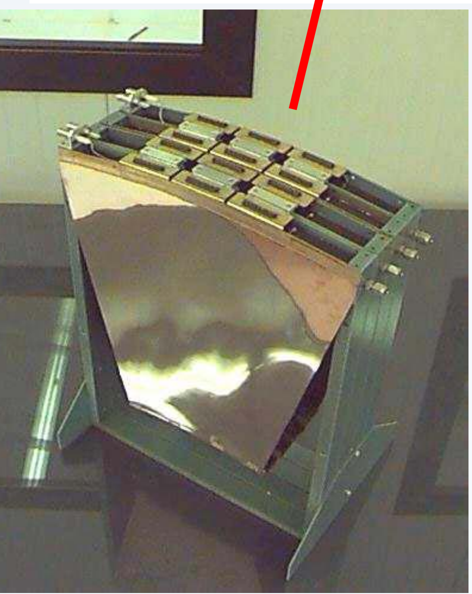

- **Straw based tracking chamber with TR capability for electron identification.**
- **Straws run in parallel to beam line.**
- **Active gas is $Xe/CO_2/O_2$ (70/27/3) operated at ~2×10^4 gas gain; drift time ~ 40ns (fast!)**
- **Counting rate ~ 6-18 MHz at LHC design luminosity 10^{34} cm^{-2}s^{-1}**

TRD detector in ALICE

Time expansion chambers
6 layers, 900 m^2

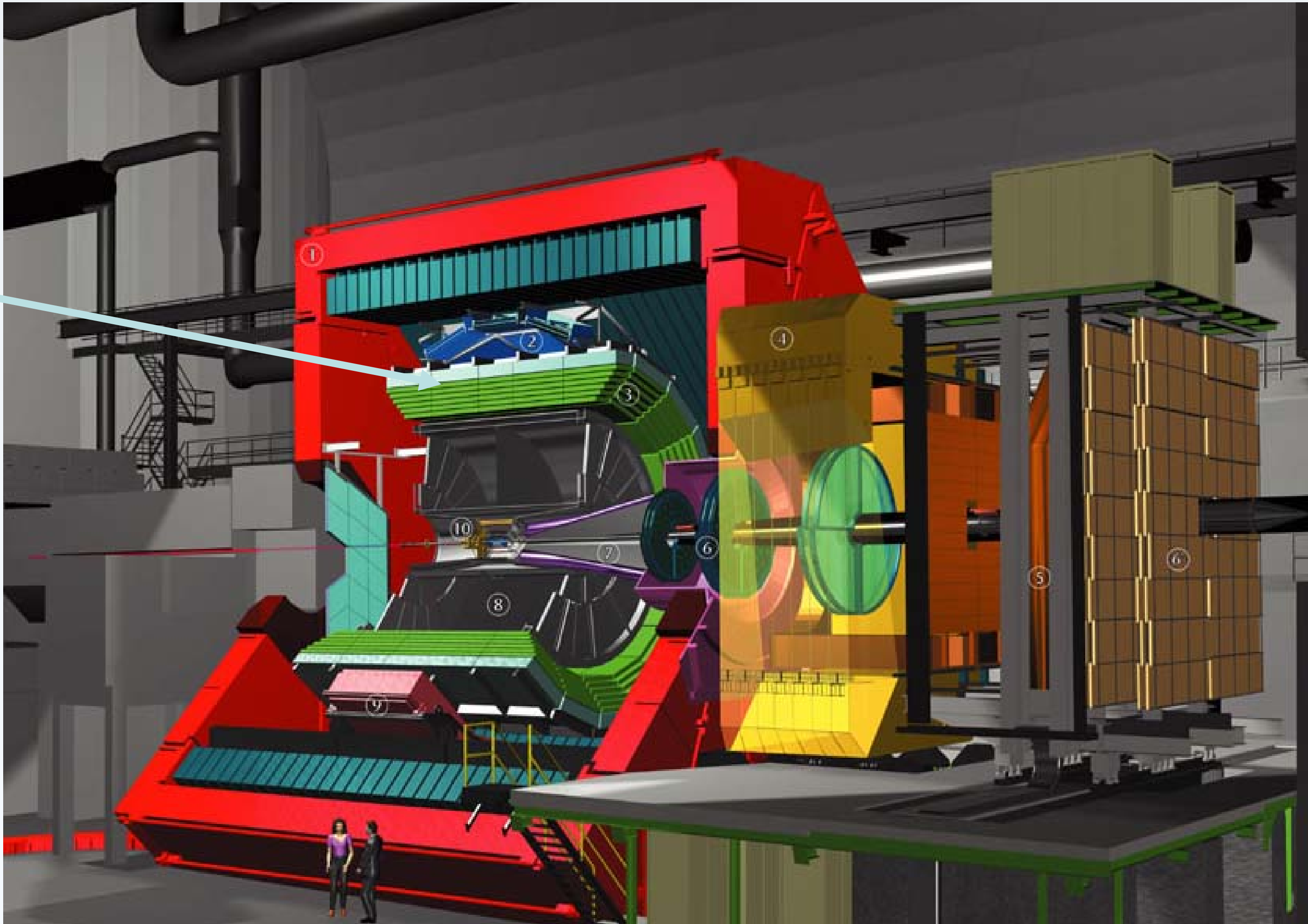

Time Expansion Chamber Principle

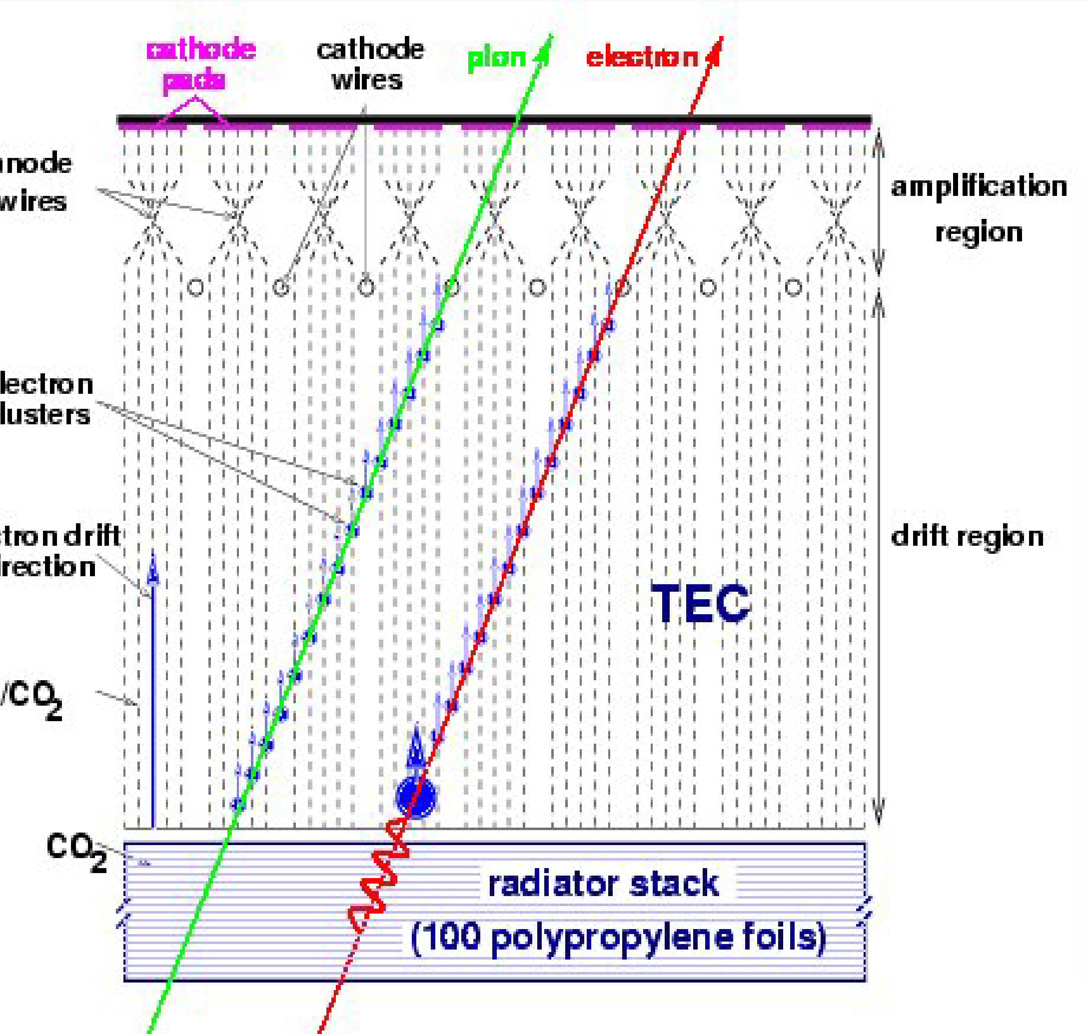

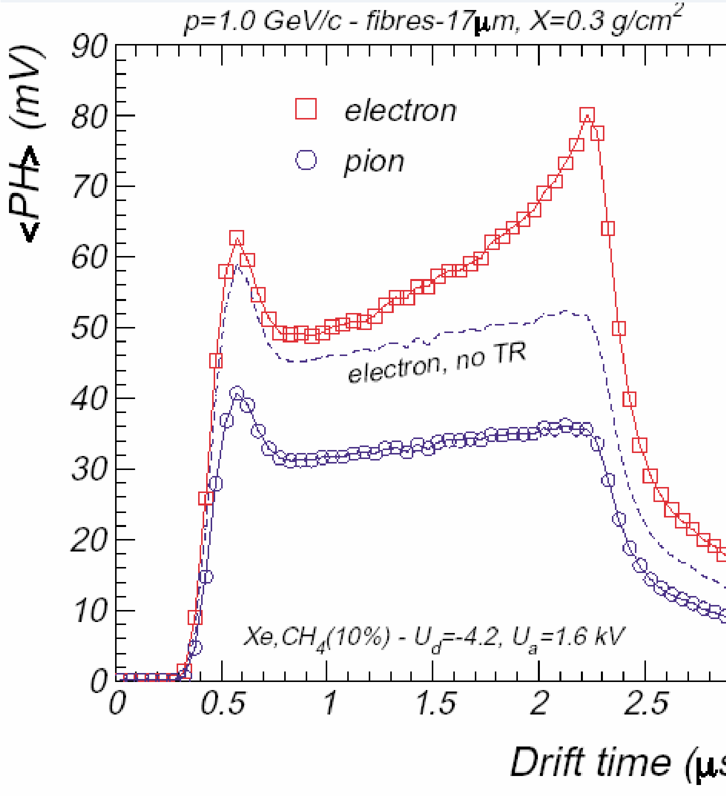

E. Napi

TRD performance